European Polymer Journal 250 (2026) 114676

Contents lists available at ScienceDirect

European Polymer Journal

journal homepage: www.elsevier.com/locate/europolj

Poly(3-hydroxybutyrate-co-3-hydroxyvalerate) quality and property control by engineering immiscible copolymer blends

Sanjay Pal [a,1], Liang-Shin Wang [a,b,1], Ana Jiménez Vergel [a], Philip Kridiotis [a], Zandrie Borneman [b], Kitty Nijmeijer [b], Alan Werker [a,c,d,*]

[a] Wetsus, European Centre of Excellence for Sustainable Water Technology, Oostergoweg 9, 8911 MA Leeuwarden, the Netherlands
[b] Membrane Materials and Processes, Department of Chemical Engineering and Chemistry, Eindhoven University of Technology, PO Box 513, 5600 MB Eindhoven, the Netherlands
[c] School of Chemical Engineering, University of Queensland, Brisbane, Australia
[d] Department of Biotechnology, Delft University of Technology, 2629 HZ Delft, the Netherlands

ARTICLE INFO

Keywords:
Polyhydroxyalkanoates (PHA)
Non-halogenated solvent recovery
Crystallinity blending
Thermo-mechanical properties
Rheology
Microstructure-property relationships

ABSTRACT

Plastic waste motivates the development of products and services from renewable, biodegradable polymers, like polyhydroxyalkanoates (PHAs). Approaches for quality control and engineering of PHA property specifications (i.e. crystallinity, crystallization rate, mechanical properties, processability, etc.) are going to be needed for industrial scale production. Methods of PHBV, poly(3-hydroxybutyrate-*co*-3-hydroxyvalerate), extraction from biomass with non-halogenated solvents were applied to formulate immiscible PHBV copolymer blends. The goal was to test, in principle, if material properties could be controlled as part of the step of PHBV extraction since solution blending is anyway inherent to the biomass extraction process. Homogenous solution blends with average 3-hydroxyvalerate (3HV) content from 0 to 38 wt% were formulated in dimethyl carbonate with proportions of the more crystalline polyhydroxybutyrate (PHB) mixed with a less crystalliine, miscible, pre-eutectic PHBV copolymer blend. Respective PHBV grade properties and microstructures were characterized using Pyrolysis GC/MS, solution rheology, DSC, DMTA, AFM, and melt rheology. Blends exhibited immiscibility (two distinct glass transition temperatures) and phase-separated microstructure morphologies (dispersed or layered-network) of interpenetrating harder and softer phases, as evidenced using Peak Force QNM. Blending systematically modulated elongation at break (from 3% to > 100%) and stiffness (from 1500 to 250 MPa). The more crystalline PHB component progressively effected melt stiffening temperature and rate, which are important to melt processing. Blending reproduced properties of an independently recovered PHBV grade with 37 wt% 3HV that was similarly independently extracted from a dried mixed microbial culture. Thus, solution blending of especially immiscible PHBV grades during PHA recovery is proposed as a novel and practical scalable route for effective property quality control and application-specific PHBV bioplastic masterbatch production.

1. Introduction

Plastic waste and its negative environmental impacts motivate regulatory and industrial developments for a greater use of biodegradable polymers, including polyhydroxyalkanoates [1,2]. Polyhydroxyalkanoates (PHAs) are a class of naturally occurring, semi-crystalline, biodegradable polyesters that are biobased renewable alternatives to conventional fossil-based thermoplastic polymers [3]. Despite PHA discovery being about 100 years ago, initiatives and investments are only more recently stepping towards wider industrial production activities to satisfy societal demands [4]. As such demands for alternatives to fossil plastics increase, fundamental developments in recent years also demonstrate increasingly both technical and economic feasibility for obtaining a wide range of possible PHAs using industrially scalable production methods [1,5–7].

PHAs are accumulated intracellularly as granules [8] by many species of naturally occurring microorganisms. Bioprocesses can generate significant amounts of PHAs using pure or mixed microbial cultures

* Corresponding author at: Wetsus, European Centre of Excellence for Sustainable Water Technology, Oostergoweg 9, 8911 MA Leeuwarden, the Netherlands.
E-mail address: alan.werker@wetsus.nl (A. Werker).
[1] Pal and Wang are co-first authors.

https://doi.org/10.1016/j.eurpolymj.2026.114676
Received 23 October 2025; Received in revised form 18 February 2026; Accepted 23 March 2026
Available online 26 March 2026

when fed organic-rich substrates, including feedstocks derived from municipal wastes and agro-industrial by-products [8–12]. Factors including but not limited to microorganism strain(s) or diversity, bioprocess cultivation conditions, and feedstock types collectively influence the as-produced grade of PHA [13–15]. Municipal and agro-industrial organic (waste) residues are readily fermentable to yield feedstocks that are dominated by volatile fatty acids (VFAs) [16]. VFAs are platform chemicals for production methods using pure or mixed microbial cultures to make PHA grades comprising copolymer blends of poly(3-hydroxybutyrate-*co*-3-hydroxyvalerate) or PHBV [17].

PHBV grade variability can arise due to inherent batch to batch quality fluctuations or as a natural result of different production methods, locations, and season. This variability can be with respect to key characteristics such as molecular weight distribution, monomer composition and its distribution, and copolymer blend composition and its distribution [2,6]. Variability in these characteristics may significantly impact the thermomechanical properties that are critical to methods and processes for making finished articles. For example, crystallization rates for the random co-polymer decrease dramatically to a minimum at the pseudo-eutectic with ≈ 50 mol % 3HV content [18]. Therefore, bioprocess production scenarios that result in biomass containing respectively distinct and/or variable grades of PHBVs will need upstream or downstream quality control methods for consistent outcomes in property specifications. Variabilities need to be accommodated to meet application specific demands for well-defined property specifications that will be required for material processability and the article performance in service [19]. Insights and reliable methods to deal with these inherent variabilities and to control the properties and the qualities of commercial PHBV grades are crucial to realize for successful industrial-scale PHBV supply chains.

PHBV granules may be recovered from a biomass by either solvent extraction or aqueous washing methods. Both methods aim to separate away the unwanted biomass and recover a purified polymer grade as the base product [8]. The recovered polymer grades are expected to be inherently copolymer blends from either pure or mixed culture production methods [20,21]. For instance, in the PHARIO project, batches of PHBV with activated sludge were produced using various sources and qualities of VFA-rich feedstocks. Regardless the respective batch of PHBV with average 3HV content, copolymer blends were miscible, but also readily fractionated into 3 dominant blend components [20]. Blends are expected because not all granules from all microorganisms in the biomass may comprise the same average monomer composition or average molecular weight. Copolymer blends are readily fractionated [21–23] due to differences in the respective fraction average monomer content and/or average molecular weight.

PHBV properties are most typically correlated to changes in average monomer composition [18]. It is also shown that distinctly different feedstock types will reproducibly produce PHBVs with predictable average co-monomer composition [24]. Average monomer composition and its distribution will influence the copolymer melt and crystallization behaviour [7,24]. However, average monomer composition does not necessarily predict polymer properties, as recently shown for mixed culture PHBV production [7]. In another example, difference in feeding strategy to produce distinctly different copolymer blends and monomer distributions resulted in one unique outcome of significantly enhanced mechanical properties of elongation at break [25]. This desirable property outcome was attributed to different phase structures that can result out of a competition between co-crystallization and phase segregation for blends of these semi-crystalline copolymers. A copolymer blend can be an inherent result of the biological and PHA extraction processes, or it can be achieved by combining PHA from different production batches. In both cases, it is a goal to generate masterbatches of polymers with controlled and consistently targeted property specifications for applications.

Melted copolymer blend components interact as a function of temperature with influence on extent of crystallinity, crystallization rates, and the resulting microstructures [26]. The PHBV copolymer blend fractions are shown to become immiscible when they differ by over about 11 wt% in average 3-hydroxyvalerate (3HV) content [20,27,28]. The role of PHBV blend components, blend distribution and miscibility, on PHBV grade processing and mechanical properties is not well described in the research literature. It is to be expected that the interplay of disparate inherent crystallization kinetics of blend components will influence resulting interactions and the integration of blend components into distinct microstructural phases depending on the blend composition, the thermal history, as well as other processing conditions [26]. However, quality control methods for engineering and systematically tuning of mixed microbial culture PHBV grade properties by purposefully making blend compositional changes in general, and particularly for immiscible blend compositions, have not yet been well-developed.

It was hypothesized that PHBV grade properties may be predictably controlled by selectively mixing proportions of distinct batches of PHBV grades having distinctly different crystallinity and crystallization rates [29]. Ultimately, since PHA solvent extraction also acts as an effective blending process, property modulation and formulation with crystallinity control can be readily accomplished directly in the extraction process. PHA-rich biomass containing varying PHA grades could be proportionally combined before the extraction process. Extraction steps would then recover engineered masterbatches of purified PHA with defined property specifications set by the pre-determined and manufactured blend composition. For the present investigation, the objective was to first evaluate if PHBV solution blending is a viable method for effectively causing systematic changes, and thereby predictable outcomes, in PHBV copolymer blend properties. Secondly, the influence of blend composition on microstructure was examined towards gaining fundamental insight on the mechanisms for how different PHBV blend components may influence the resulting polymer properties.

A set of PHBV copolymer blends were prepared from 0 to 38 wt% average 3HV content. Dimethyl carbonate solution blending methods were applied to mix selected proportions of a more crystalline PHB homopolymer (0 wt% 3HV) with a less crystalline PHBV as-produced copolymer blend (38 wt% 3HV). The applied solution blending approach was selected because it was compatible with methods and principles of PHA extraction from biomass when using non-halogenated solvents [30]. The blend properties were compared with respect to properties of an as produced and distinctly different PHBV grade (37 wt % 3HV) that was similarly and independently extracted from a mixed culture biomass at pilot scale. This reference PHBV grade was also a copolymer blend. Trends in the properties of respective newly formulated solution blended PHBV grades were evaluated to test an ability to tailor thermomechanical properties in masterbatches of recovered PHBVs. Thermal, rheological, mechanical, and microstructural properties of the formulated PHBV grades were studied and compared. Outcomes of the blend miscibility and resulting thermo-mechanical behaviours were evaluated based on interpreted microstructure-property relationships and known principles for thermoplastic elastomers. The study objective was to advance fundamental insights and to develop strategies for industrial scale polymer property specification quality control with a focus on mixed microbial culture PHBV production and its recovery.

2. Materials and methods

2.1. PHA types and sources

Three distinct PHBV grades were used, including two derived from mixed microbial culture (MMC) and one from pure culture production methods. Batches of MMC PHBV were produced in pilot scale reactors using direct accumulation bioprocess methods [6,7] with municipal waste-activated sludge, as part of the PHARIO (2015) and SCALIBUR (2020) projects [7,24]. The PHBV was available from PHARIO or SCALIBUR projects as batches of dried PHA-rich biomass. Each batch

represented an independent production run with respectively different PHBV grades due to the different feedstocks used. The PHBVs from selected batches were recovered at pilot scale to greater than 98% purity (determined by TGA) using 2-butanol (98% pure, VWR Chemicals, the Netherlands) in a 10-L extraction vessel as previously reported in detail [30,31]. For the purposes of the present investigation, a batch of PHARIO PHBV with 38% wt. average 3HV content (determined using PyGCMS) was used for the blending study. This PHARIO PHBV was produced on a primary sludge fermentate [20]. A distinct SCALIBUR PHBV batch with 37%wt. average 3HV content (determined using PyGCMS) was used as a target quality reference polymer. This SCALIBUR PHBV was produced on a 76:24 mixture (COD basis) of acetic and propionic acids to explicitly result in a PHBV with similar average 3HV content as the PHARIO PHBV used in this study [7].

The pure culture produced commercial homopolymer polyhydroxybutyrate (PHB) (98% pure with 0 wt% 3HV and without additives) from Biomer (Germany) was solution blended with PHARIO PHBV to evaluate potential for engineering of copolymer blend properties.

2.2. Solution blending

A series of eight blends with proportions of PHB and PHARIO PHBV were prepared and defined according to the weight percent of PHB that was used in the blend from 0 to 100 wt% PHB. Replicate (n = 4) weighed proportions of PHB and PHBV to a total weight of 0.5 g were combined with 13 mL dimethyl carbonate (DMC, 99% pure, Thermo-Scientific Chemicals, The Netherlands) in 16.5 mL glass test tubes (LZP065, Hach™, United States). Test tubes were sealed and heated to 140 °C (QBH2, Grant, United Kingdom) with periodic vortex mixing over 30 min to form well-mixed polymer solutions. This procedure effectively mimicked demonstrated methods of PHA extraction from biomass using non-halogenated solvents, including 2-butanol and DMC [31]. The solutions were cooled to 80 °C, transferred to Petri dishes, and dried by vacuum oven at 40 °C over 48 h (0.2 bar, 3.5 L/min N_2 gas flow).

2.3. Analytical methods

2.3.1. Pyrolysis with gas chromatography (PyGCMS)

PHBV monomer compositions were determined by pyrolysis with gas chromatography (GC, HP Agilent 6890 N, Agilent Technologies, United States) and mass spectroscopy (MS, Agilent 5975 XL Mass Selective Detector, Agilent Technologies, United States) using a pyrolysis thermal decomposition system (PYRO, Gerstel GmbH, Germany). Representative 50–125 μg grab samples from the blends were used for measurements made according to methods as previously described [31].

2.3.2. Differential scanning calorimetry (DSC)

DSC (DSC 3+, Mettler-Toledo, Switzerland) was performed with 2–3 mg polymer samples under nitrogen flow (50 mL/min). Tared samples were brought to –70 °C for 5 min, followed by: (ramp 1) heating from –70 °C to 190 °C at 10 °C/min, holding for 30 s, and quenching at –100 °C/min to –70 °C, and (ramp 2) heating from –70 °C to 190 °C at 10 °C/min, holding for 30 s, and quenching at –10 °C/min to –70 °C. After ramp 2, the samples were aged at room temperature and assessed again after 1 month with the same method. The reported polymer (maximum) melt enthalpy and melt temperature (T_m) was determined from ramp 1 of the aged sample. The glass transition was assessed from ramp 2. Crystallization was assessed based on the quenching applied after ramp 2. The onset and peak crystallization temperatures and the difference between the onset and offset temperatures were reported. Analyses were made with Mettler-Toledo STARe evaluation software (Version 16.4) and in-house analytical software tools written with MATLAB (R2022a).

2.3.3. Thermal gravimetric analysis (TGA)

PHA content (g PHA/g biomass) and purity (g PHA/g sample) were determined by thermal gravimetric analysis (TGA 2, Mettler-Toledo, Switzerland) as previously described [31]. 4–5 mg of ground biomass, polymer powder or cut films were used for each measurement in tared ceramic crucibles. Weight loss was followed after sample insertion at 80 °C (50 mL/min N_2 flow) followed by heating at 10 °C/min to 105 °C. After isothermal drying at 105 °C for 10 min, heating was continued at 10 °C/min (50 mL/min N_2 flow) to 550 °C. Finally isothermal incubation was maintained for 30 min at 550 °C (50 mL/min air flow) for sample ashing.

2.3.4. Solution rheology

Concentric cylinder solution rheology (MCR 102 with a CC17, Anton Paar GmbH, Austria) was used to measure viscosity of 5 mL of nominally 15 mg/L polymer sample solutions in DMC at 60 °C with 75 s^{-1} shear rate, as previously reported [31]. 10 mL solutions were prepared in DMC by heating weighed polymer and solvent in sealed tubes (LZP065, Hach™, United States) to 140 °C for 10 min before cooling and maintaining at 70 °C pending rheometer measurements. An average viscosity with confirmed solution stability was determined for each sample over 5 min of constant applied shear rate with time-averaged viscosity logged every 10 s. An intrinsic viscosity [η] (in dL/g) was estimated based on the Solomon-Ciuta equation [32]. Intrinsic viscosity was related to the polymer weight average molecular mass (M_w) with the Mark-Houwink equation:

$$[\eta] = K \cdot M_w^{\alpha} \tag{1}$$

Methods of heat treatment were applied for the PHARIO PHBV and for PHB as previously reported [31] to estimate the Mark-Houwink constants (K, α) of (0.010, 0.740) and (0.021, 0.651) for PHARIO PHBV and PHB, respectively.

2.3.5. Melt rheology

Parallel plate melt rheology (MCR 102 with a PP25, Anton Paar GmbH, Austria) was performed on the polymer samples. Dried 0.25 ± 0.02 g grab samples were pre-formed into ∅ 25 mm diameter coupons. Coupons were formed in a stainless-steel mould at room temperature with a five metric ton load applied over five minutes by hydraulic press. Rheology analysis was initiated by first heating coupons to 195 °C and pressing for 2 min with 25 N normal force. Three measurement segments were then performed with 10 N normal force and 2% strain in oscillatory shear: 1) 2.25 min isothermal at 195 °C and 1 Hz, 2) 10 min frequency sweep at 195 °C from 0.1 to 100 Hz, and 3) 12.5 min quenching from 195 to 15 °C 1 Hz. Viscoelastic properties were logged with 7.5-second time-averaging.

2.3.6. Dynamic thermomechanical analysis (DMTA) and mechanical testing

Solution-cast specimens were prepared from 50 mg samples that were first dissolved in 10 mL DMC in sealed test tubes (LZP065, Hach™, United States) at 140 °C for 10 min in a heating block (QBH2, Grant, United Kingdom). The solution was then transferred to a second heating block at 80 °C for 15 min before pouring the solution into a heated (75 °C) petri dish (94ø mm, 20 mm height, Duroplan®, DURAN®, DWK Life Sciences, Germany). The solvent was evaporated completely under N_2 atmosphere overnight. The resulting films were carefully peeled away from the petri dish and aged at room temperature for one week wherein crystallization developments have been previously measured to take about 3 days [31]. Mechanical testing and dynamic thermomechanical analysis were performed on rectangular test specimens (5.3 × 8 mm) that were cut from solution-cast films. Film thickness was measured for each specimen with a digital gauge (Absolute 547-401, Mitutoyo, Japan).

Specimens were mounted for DMTA (DMA Q800 V21.3, TA Instruments, United States) and clamped with 0.9 N.m. A DMTA temperature sweep was performed from −20 to 150 °C at 3 °C/min at 1 Hz with

15 μm amplitude. Storage and loss modulus data were acquired with Universal Analysis 2000 version 4.5A. Specimens were similarly mounted for uniaxial tensile testing on the same equipment. Stress was applied with a constant displacement rate (160 μm/min, 2%/min strain rate) to a maximum displacement of 10 mm.

2.3.7. Atomic force microscopy (AFM)

Compression-moulded discs (25ø mm diameter and 1 mm thickness) were prepared using a three-plate mould in a hot press (Modell Labo-Press P300S, VOGT Labormaschinen GmbH, Germany). 0.5 g samples were compressed for 2 min at 185 °C and with 5 MPa pressure. The hot press and the mould were cooled under the applied pressure with a continuous tap water supply until the mould reached ambient temperature. The discs were then annealed for 48 h at 40 °C under nitrogen atmosphere.

AFM (Dimension Icon, Brucker, United States) was performed on discs using Nanoscope software (Version 8.15). A TESPA cantilever probe was used (Length: 110–140 μm, Width: 25–35 μm, Thickness: 3.5 – 4.5 μm, frequency f_0: 245 – 327 kHz, spring constant k: 20 – 80 N/m, and tip radius: ~8 nm). PeakForce QNM (Quantitative Nanomechanics) mode was applied for acquiring images of height topography with nanomechanical mapping of stiffness, adhesion, and deformation. The probe cantilever was calibrated by the absolute calibration method, and the probe deflection sensitivity was calculated by a single ramp of a 0 nm scan size on a clean sapphire standard (Veeco Peak Force QNM sample kit, Bruker, United States) with recommended parameters according to the PeakForce QNM user guide (004–1036-000, [33]). The spring constant of the probe was estimated by the thermal tune function in the Nanoscope software with a Lorentzian model to fit the resonance peak. The 8 nm probe tip radius was specified by the manufacturer, and this radius was used for the calibration. Captured images were processed and analysed by Gwydion software (version 2.65).

Measurements were performed on the annealed disc surfaces at 1 Hz and 512 lines per reading over 100 and 6.25 sq. μm scan areas giving stiffness-mapped images with 512 X 512 pixels in dimension. The root mean square (RMS) stiffness (Sq) was calculated based on the i^{th} stiffness (z_i) and average stiffness ($\bar{z}$) values corresponding to the oscillating signals converted to colour images that mapped between minimum and maximum stiffness values for each scan:

$$\textit{Average stiffness} \quad \bar{z} = \frac{1}{N}\sum_{i=1}^{N} z_i \tag{2}$$

$$\textit{RMS stiffness} \quad S_q = \sqrt{\frac{1}{N}\sum_{i=1}^{N}(z_i - \bar{z})^2} \tag{3}$$

where N is the total number of mapped points for the scan. RMS stiffness values were estimated for at least 3 scans from different locations for each sample. Average RMS stiffnesses were compared between the different blend compositions. A polystyrene standard (Veeco Peak Force QNM sample kit, Bruker, United States) was scanned as a reference sample for which S_q was 4.9 ± 4.1 GPa (n = 6) [33]. A compromise was made due to an interest to use the same tip for all measurements. The selected tip was more suited for relatively softer materials (i.e. the PHA blends with lower PHB content). More measurement variability resulted between replicate analyses of the stiffer PHB samples and for the polystyrene standard.

3. Results and discussion

3.1. Feedstocks influence the as produced PHBV copolymer blend quality

The thermo-mechanical properties of mixed culture PHBV copolymers are typically considered only with respect to the average 3HV content. The research literature generally neglects contribution of copolymer blend distribution to microstructure developments and the resulting material properties [18,34], except, for example, when non-random co-polymers are produced on purpose [17]. Batches of dried PHA-rich biomass were acquired during PHARIO [24] and SCALIBUR (www.scalibur.eu) [7] in pilot scale projects by methods of direct accumulation using the same source of municipal waste-activated sludge in 2015 and 2020. Despite differences in production date, scale, and production facilities, with campaigns performed during all seasons, the outcomes of recovered average monomer composition were robust and predictably a function of the organic composition of the feedstock [7]. For example, a feedstock mixture of acetic and propionic acids (the SCALIBUR PHBV used in this study) could be selected to predictably and reproducibly yield a grade of PHBV with very similar average monomer composition of the PHARIO PHBV. This particular PHARIO PHBV was similarly robustly produced on fermented primary sludge. All other factors including the bioprocess methods and biomass source were the same. However, even if PHBV grades with similar predictable average monomer contents could be obtained, average 3HV content alone was found not to be sufficient to predict the polymer properties [7].

PHARIO and SCALIBUR PHBV grades used for this study have similar average 3HV contents, and molecular weight (Table 1), but they are distinct in thermo-mechanical properties [24,35]. These differences were interpreted to be due to respective feedstock-dependent bioprocess influences that promoted for different outcomes in the resulting copolymer blend distributions extracted from the respective production batches of dried biomass [20]. All PHARIO PHBV production batches in general (59 batches, 3 distinct feedstocks) were found to be miscible copolymer blends with 3HV content varying predictably from 0 to 45 wt % as a function of feedstock organic composition [13,24].

Characterization of activated sludge mixed culture PHBVs was undertaken in PHARIO [20]. Insights and methods of molecular weight control have been further developed [31]. Conditions of mixed culture production were the same for SCALIBUR except for controlled rapid drying of the harvested biomass to avoid undue polymer decomposition and loss in molecular weight [7]. A polydispersity index (Đ) of about 2 has been routinely obtained for the applied production methods, as demonstrated in production campaigns performed over more than 1 year [20]. The expectation of Đ ≈ 2 is based on theoretically predicted outcomes for step-growth linear polymerization [36,37]. It is also found that thermal decomposition by heat treatment, storage of the dried biomass for several years, or extraction in so-called PHA-poor solvents do not result in significant changes in Đ, even if there may be some molecular weight loss due to random scission [20,31]. During PHARIO, melt rheology was used to estimate M_w in routine characterization because GPC was found to become increasingly more problematic to perform especially for the more crystalline PHBVs (lower 3HV contents) with M_w values towards and above 1000 kDa [38]. Solution rheology methods for M_w estimation using DMC were developed to enable measurements using less sample mass than is required for melt rheology [31]. The Mark-Houwink estimated M_w for the samples via solution rheology in the present work were corroborated with selected samples analysed externally with GPC.

PHB homopolymers and PHBV copolymers have similar structures. However, the longer or shorter side chain can lead to different free-volume packing [27] and will influence the extent of crystallization and the crystallization rates for these copolymer blends [26]. PHARIO PHBVs can be fractionated into at least 3 main components with chloroform-hexane precipitation methods [20]. In fractionation experiments, components precipitate as a function of the respective component average M_w and average 3HV content.

For miscible PHBV copolymer blends, DSC heating ramps on aged microstructures reveal broad melting peaks. For PHBV copolymers blends beyond about 10 wt% average 3HV content, compositional distribution was broad, as evidenced by uninterrupted melting peaks from 50 to 180 °C [20]. Thus, the blend character is reflected in the melt enthalpy distribution including start and end temperatures together

Table 1
Summary of the characteristics for PHB, PHARIO, and SCALIBUR PHBV. Subscripts d, m, g, and c denote decomposition, melt, glass transition, and crystallization onset temperatures, respectively. ND is not detectable.

Sample	3HV content [wt.%]	[η] [dL/g]	M_w [kDa]	Purity [%]	T_d [°C]	T_m [°C]	ΔH_m [J/g]	T_g [°C]	T_c [°C]
PHB	0	1.7	830	98	287	168	131	4.0	116
SCALIBUR	37	1.5	917	98	297	134	73	−4.8/3.8	88
PHARIO	38	1.3	756	99	297	92	58	−2.7	ND

with the corresponding shift in the melting temperature (T_{m50}) at median peak enthalpy in line with founding observations in studies of PHBV blends [27,28]. The SCALIBUR PHBV was confirmed as a copolymer blend by solvent extractions from replicate batches of SCALIBUR PHBV-rich biomass in DMC [7]. For two such replicate production batches, a crude fractionation was performed. Extraction was followed by selective rapid gelation and separation of the more crystalline blend component by addition of 2-butanol to the hot DMC solution (1:2 v/v). The selectively recovered blend component represented 58 ± 1 wt% of the PHBV mass, with 23 wt% 3HV versus 47 wt% for the remaining still soluble component as estimated from a mass balance. The broad separation in average monomer composition for the two resolved components supported the observation of two distinct glass transitions for an immiscible SCALIBUR PHBV copolymer blend as discussed below.

In previous work, miscible and immiscible binary and ternary blends were fabricated by recombining PHBV blend fractions in either their original or different proportions [20]. From these results, criteria were established for immiscible 'mixed-culture' PHBV copolymer blends. Components became immiscible when the 'extreme' fractions were not bridged by an 'intermediate' blend component wherein the 'extreme' fractions differed by more than 11 wt% in average 3HV content. These criteria for immiscible PHBV copolymer blends derived from diverse mixed culture systems agreed well with earlier literature findings made with pure-culture PHBV copolymer blends [28]. However, the inherent blend quality of PHA copolymers produced with either pure or mixed culture methods is unfortunately not typically evaluated in the research literature. Instead, PHAs are produced and reported in research studies often with only results of the average monomer composition implying an assumed 'pseudo' copolymer.

Miscibility and immiscibility of the PHARIO and SCALIBUR PHBV copolymer blends are therefore indicated by the single or double resolved glass transition (T_g) temperatures (Fig. 1). A single T_g is expected when the 'adjacent' dominant blend components do not differ by more than about 11 wt% in average 3HV content [20]. The trend in T_g for miscible copolymer blends has correlated directly to the recovered PHBV average 3HV content and followed the Fox equation for T_g [18,39]. Contrary to the PHARIO findings, SCALIBUR PHBV

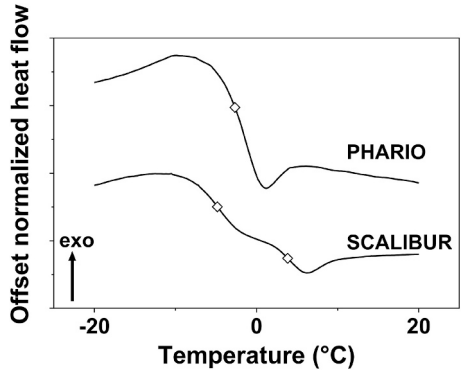

Fig. 1. DSC heat flow trends contrasting glass transitions for the PHARIO versus SCALIBUR PHBV grades recovered from biomass batches after direct accumulation using municipal activated sludge (Table 1). White diamonds indicate the glass transition temperature(s).

accumulations unexpectedly and reproducibly resulted in recovered PHBV grades with two distinct glass transition temperatures (Fig. 1). Thus, for the SCALIBUR PHBV-rich biomass, a distribution of PHA granules in the dried biomass between or within the microorganisms contributed to inherently form an extracted immiscible copolymer blend. These PHBV copolymer blends, recovered by solvent extraction using 2-butanol, have two dominant immiscible phase-separated PHBV components without a bridging component.

An effect of immiscibility for PHBV copolymer blends on crystallization onset and microstructure developments was further seen from AFM stiffness mapping (Fig. 2). Given the same processing conditions to make the sample discs, the AFM scans for the PHARIO PHBV grade revealed a uniform single-phase microstructure morphology (Fig. 2b). On the other hand, the SCALIBUR PHBV grade resulted in an immiscible hard and soft phase-separated layered-network biphasic microstructure (Fig. 2a, left). This biphasic morphology was fit to a bimodal Gaussian stiffness distribution, where bimodal peaks were clearly observed (Fig. 2a, right). Interestingly, in spite of the similar 3HV contents, SCALIBUR PHBV also exhibited higher extent of crystallinity (Table 1) and superior toughness from mechanical testing (section 3.3) compared to the PHARIO PHBV. Under the same conditions of cooling from the melt, SCALIBUR PHBV exhibited a detectable crystallization peak with crystallization onset temperature of 88 °C, while similar pre-eutectic PHARIO PHBV did not. It was hypothesized that higher extent of crystallinity and the more readily crystallizable nature for SCALIBUR PHBV was due to the phase separated component with lower average 3HV content and, thus with crystallization behaviour more like the homopolymer PHB. The enhanced mechanical properties of SCALIBUR PHBV were interpreted to be microstructure-property related. Given that the 3HV monomer can be accommodated within a PHB lattice [18], the phase interfacial regions are likely to be part of a interpenetrating polymer network. The material behaviour was interpreted to be a direct consequence of the unique copolymer immiscible blend distribution defined by two main components of sufficiently widely separated average 3HV contents with respective differences of inherent extent of crystallinity, crystallization temperatures, and crystallization rates. Co-crystallization gave an intermixed microstructure network with phase-separated 'harder' and 'softer' regions that are likely dominated by the respective more rapidly and less rapidly crystallizing blend components. The hard regions will contribute to properties of strength and rigidity, while the network of interconnected soft regions, if entangled with the hard regions, will impart matrix properties of flexibility and toughness.

An ability to formulate distinct blends with addition of more readily crystallizable components, thereby influencing onset crystallization and microstructural development due to co-crystallization, would enable a means to tailor PHBV grade properties. PHBV grades can be tuned according to processing or application requirements in a way that offers a unique degree of freedom for property modulation in extension to the bioprocess alone. Blending in solutions can be effectively accomplished without need for melt processing because it is inherent to the steps of extraction in downstream processing for solvent-based methods of PHA recovery [40].

It was therefore hypothesized that biphasic microstructures like this SCALIBUR PHBV should be possible to reproduce by solution blending selected proportions of batches of PHBV grades that are distinct in

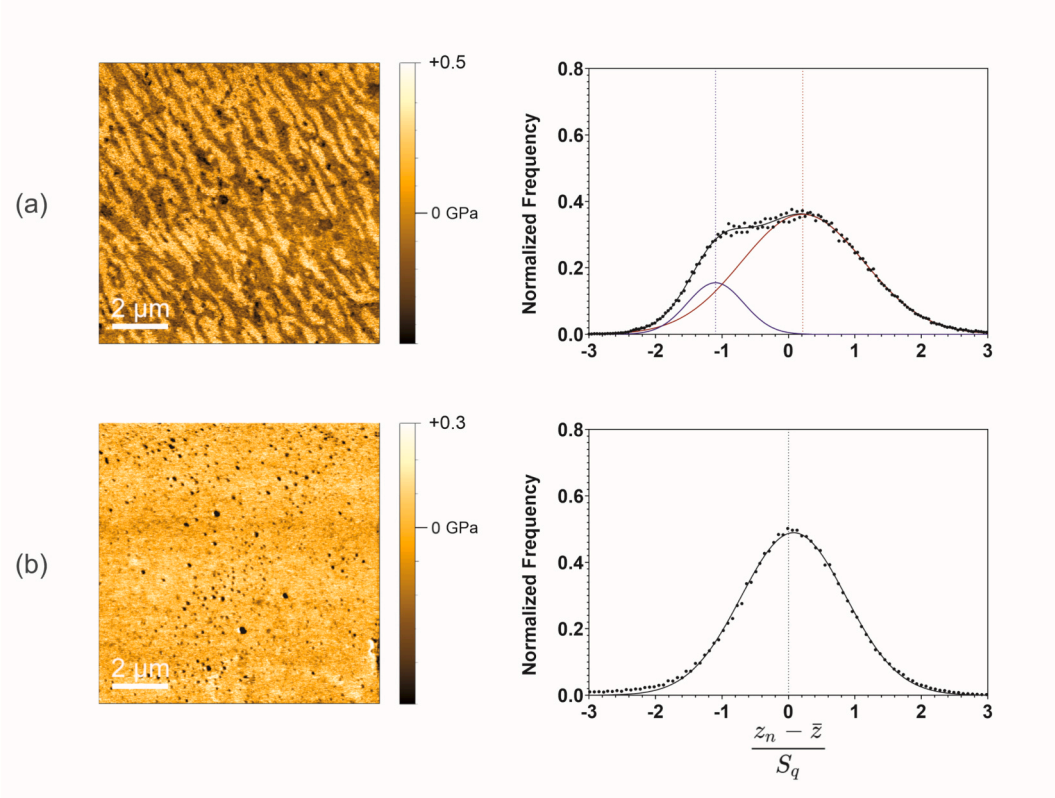

Fig. 2. PeakForce QNM stiffness maps (scan size 10 μm) and stiffness distribution-histogram plots. The colour contrast directly reflects different stiffness, where darker and lighter regions are softer and harder phases, respectively. (a) SCALIBUR PHBV exhibits a layered-network biphasic morphology (estimated as a bimodal Gaussian stiffness distribution with red and blue line indicating individual peak locations), and (b) PHARIO PHBV exhibits a single-phase morphology (estimated as a Gaussian stiffness distribution).

respective extents of crystallinity. This hypothesis was tested in the subsequent reported blending experiments. A series of controlled masterbatches of formulated PHBV copolymer blend grades were produced by solution blending different proportions of the more crystalline commercial PHB with the less crystalline grade of PHARIO PHBV.

3.2. Blending experiment to engineer phase-separated PHBV microstructures

Eight binary PHB and PHARIO PHBV blends from 0 to 100 wt% PHB were produced (Fig. 3). The regression line between the expected (mass balance) 3HV contents and the respectively measured (PyGCMS) values support that solution blending resulted in reasonably consistent

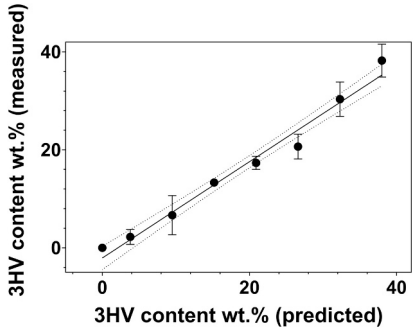

Fig. 3. Average monomer compositions for a series of eight formulated PHB and PHARIO PHBV copolymer blends. Replicate (n = 3) measured 3HV contents by PyGCMS are reported with respect to the values predicted from mass balances. The solid line is the linear regression with 95% CI bands shown (slope = 0.98 ± 0.1).

outcomes in the average 3HV comonomer composition. No significant difference between measured and expected average 3HV contents in replicate measurements from small microgram grab subsamples were observed, supporting the hypothesis that both PHB and PHARIO PHBV were dissolved and well-mixed under the conditions applied for the solution blending process.

Blend quality was assessed with respect to molecular weight (intrinsic viscosity) and glass transition temperature(s) (Fig. 4). Fig. 4a shows the intrinsic viscosity as a function of the blend PHB weight fraction. The PHB had higher intrinsic viscosity than the PHARIO PHBV (Table 1). Intrinsic viscosity differences are expected due to differences in average molecular weight and/or differences in polymer coil geometry or interactions reflected, for example, by the Mark-Houwink constants [31]. Intrinsic viscosity increased linearly based on blend proportions, as expected and as reported in the literature for immiscible PHBV blends [28]. However, the blend values all deviated down from expectations based on the interpolated (mass balance) intrinsic viscosities for the compositions (solid line in Fig. 4a). The trend for the expected blend mass balance intrinsic viscosities fell outside the 95% confidence interval (CI) of the linear regression line expressed by the blends. This outcome suggests interactions of the dissolved polymer coils in dilute solution with the development of intermingled coils of the two main blend components. Interaction between copolymers of PHBV and PHB molecules in solution would contribute to an effective reduction of hydrodynamic volume and/or number of independent coils, resulting in a reduced intrinsic viscosity [41]. This indication for an effect of coil interaction from the solution rheology provided a first sign for a tendency for formation of interacting and interpenetrating polymer networks at the interface of a biphasic microstructure as further discussed in section 3.4 with AFM results.

Two distinct glass transition temperatures were detected for all the

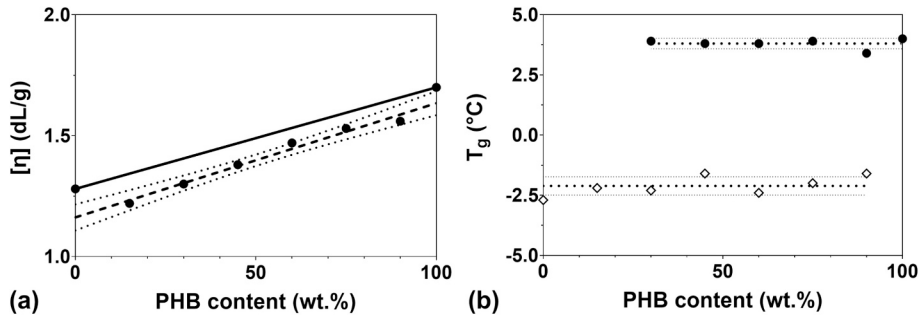

Fig. 4. (a) Intrinsic viscosity (●) for the PHB and PHARIO PHBV grades, and the blends. The linear regression of [η] for the blends (dashed line) with 95% CI bands (dotted lines) falls below the expected values based on interpolation from the respective components (solid line). (b) Average glass transition temperature(s) (T_g) for each blend (dashed line) with 95% CI bands (dotted lines). Solid black dots reflect T_g corresponding to PHB portion, and the diamonds correspond to PHARIO PHBV.

binary blends except for the blend with 15 wt% PHB (Fig. 4b). In this case of lower blend PHB content, the T_g corresponding to PHB may have been difficult to detect due to phase interactions and a lower baseline signal shift from the relatively smaller mass of PHB in the sample. Otherwise, detected T_g values on average reflected the respective blend component values of 3.8 ± 0.2 (PHB) and −2.1 ± 0.4 °C (PHARIO PHBV) with no significant influence of blend composition. Apparently, upon rapidly quenching (−100 °C/min) such immiscible copolymer blends, the resulting amorphous microstructures are resolved into phases of the blend components as distinct from one and the other. This outcome demonstrates that these phase-separated copolymer blends contained two dominant components, similar to those inherently produced in the case of SCALIBUR PHBV. Immiscible copolymer blends can be recovered from a biomass produced in a batch bioprocess or they can be generated as part of the downstream solution blending of distinct batches in the PHA recovery. SCALIBUR PHBV also has two T_g steps. One reflects a T_g of effectively PHB (3.8 °C), and the other (−4.8 °C) represents a copolymer blend fraction with lower extent of crystallinity and higher average 3HV content (Fig. 1). According to the Fox equation, a linear dependence of T_g with average 3HV content is expected for miscible PHBV copolymer blends [20,24]. From the current work (Fig. 4b), such a correlation would suggest the less crystalline blend component in SCALIBUR PHBV to be in the order of 50 average wt.% 3HV (SI 1.4). Then from a mass balance (Fig. 3), the resulting effective PHB content for SCALIBUR PHBV may be expected to be in the order of 26 wt% PHB. This prediction fits with the crude fractionation that was performed (Section 3.1) with 2-butanol in DMC. The less crystalline blend component remaining in solution was estimated to be about 47 wt % 3HV.

Like the observations for glass transition, all samples revealed two distinct melting clusters for the aged microstructures (Fig. 5a). No detectable intermediate peaks were observed between these two

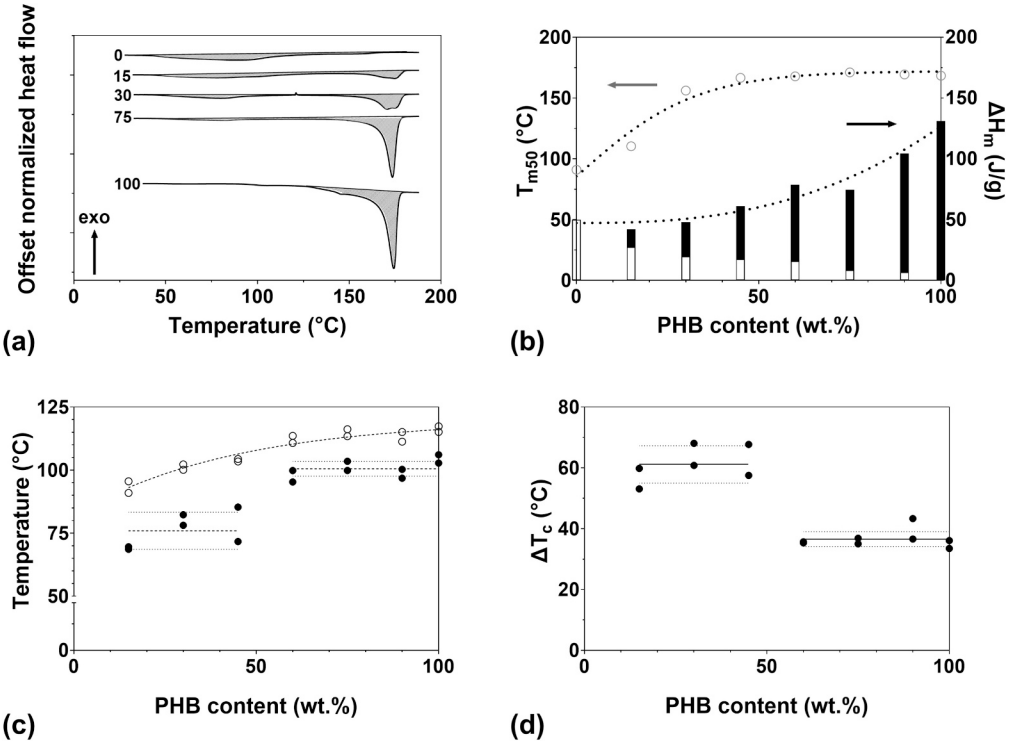

Fig. 5. (a) DSC thermographs of 1-month aged PHB and PHARIO PHBV blends ranging from 0 to 100 wt.%PHB (ramp 1, 10 °C/min), (b) T_{m50} (median melting temperature) from the melting peak (left axis, open circles), ΔH_m (melt enthalpies, right axis) corresponding to less crystalline component (white bars) and more crystalline component (black bars) versus PHB content in the respective blends. (c) Crystallization peaks arising during the 2nd quenching scan (−10 °C/min). White dots represent the crystallization onset temperatures. Black dots represent the crystallization peak temperatures. No crystallization peak was detectable for PHARIO PHBV (i.e. 0 wt% PHB blend) (d) ΔT_c is the difference between the crystallization peak onset and end temperatures.

'unbridged' separated melt enthalpy regions. A phase corresponding to the less crystalline PHARIO PHBV consistently exhibits a broad melting peak with a T_{m50_1} centred at 80 ± 6 °C. This lower temperature melting phase is not present directly after the second heating scan due to the slow crystallization rate for this blend component (Fig. S1a). Disparity of crystallization rates between blend components is believed to be an important contributing factor for the characteristic developments in microstructure formation for these blends. The more crystalline PHB component contributes to the second phase that melted at a significantly higher temperature range (T_{m50_2}: 170 ± 1 °C). Aged microstructures of miscible PHBV random copolymer blends have been previously shown to exhibit a median melting temperature (T_{m50}) that is directly proportional to the copolymer blend weight average 3HV content [20]. However, Fig. 5b shows that such a relationship is not followed in the case of immiscible PHBV copolymer blends. The T_{m50} for these immiscible PHBV copolymer blends gave the weighting of the melt enthalpy balance from the more and less crystalline phases. Above 50 wt% PHB in the formulated blends, T_{m50} increases from 90 to an asymptote of 171 °C. Beyond 50 wt% PHB, T_{m50} is dominated by the enthalpy of the more crystalline PHB phase. This relationship was also further supported by the portion of melt enthalpies corresponding to more and less crystalline phases, as discussed below.

Unlike the glass transition temperatures for the immiscible amorphous phases formed after quenching, the aged and crystallized microstructures did reveal a systematic effect related to the blend composition. Evidently, the PHARIO PHBV blend component interferes with the PHB component to crystallize because the overall melt enthalpy did not increase progressively with the blend composition (Fig. 5b). The blending influence on extent of crystallinity was non-linear and started at a plateau melt enthalpy (61 ± 1.8 J/g) before following a second order increasing trend, beyond 50 wt% PHB content, to the limiting value for PHB. Suppression of the inherent PHB crystallization rate provides time for the development of more complex microstructures that can incorporate elements of the less crystalline, more slowly crystallizing, PHARIO PHBV copolymers. It was of particular interest to observe that influence of the PHARIO PHBV on PHB crystallization was sustained over such a wide range of blend compositions (from 0 to ≈ 50 wt% PHBV). This crystallization retardation factor further supports that interpenetrating zones can develop, given time for possible diffusion, intermixing, incorporation, and interlocking of less crystalline higher 3HV polymer chains into a crystallizing matrix driven by the more crystalline PHB polymer chains. Even if two distinct microstructure domains are formed, interactions between PHARIO PHBV and PHB are understood to have been significant from Fig. 5b.

The interactions between these less and more crystalline blend components must influence nucleation and crystallization rates for the blends [42]. A 50 wt% PHB content was a threshold for a shift in the melt crystallization behaviour (Fig. 5c and Fig. 5d). The pre-eutectic PHARIO PHBV is known to exhibit a slow crystallization process [31], and in this case there was no detectable crystallization during quenching at −10 °C/min. As blend PHB content increased, a crystallization peak progressively emerged as expected (Fig. S1b). The enthalpy of crystallization increased progressively (Fig. S1c), reflecting an expected increase in crystallization tendency in proportion to the added PHB weight fraction.

While the crystallization peak temperatures exhibit a step change from 76 ± 7 °C (n = 3) at below 50 wt% PHB to 101 ± 3 °C (n = 4), the onset temperatures show a more pronounced initial increase, followed by a more gradual trend (Fig. 5c). The higher onset crystallization temperatures indicate an earlier onset for crystallization with a stronger driving force for nucleation. For blends containing less than 50 wt% PHB, more crystallizable islands are anticipated to form and to become intermixed within a predominant very slowly crystallizing PHARIO PHBV domain. The much more readily crystallizable phases could act as initial nucleation sites, initiating crystallization while being hindered at the same time [42]. In contrast, when the slowly crystallizable PHARIO PHBV domains are minor components, nucleation sites are formed more readily, and crystallization ensues toward the onset temperature of pure PHB.

Moreover, crystallization is a kinetic process involving nucleation and crystal growth as a function of temperature. The underlying mechanisms of the crystallization kinetics unfortunately could not be ascertained due to a limitation of applying a non-isothermal crystallization measurement using DSC. However, differences in crystallization rate behaviour between the blends can be evaluated relatively given the same applied conditions of the thermal history. The width of the crystallization peak is shown as the temperature difference (ΔT_c) between the onset and end of crystallization (Fig. 5d). Given the same cooling rate (−10 °C/min), lower ΔT_c indicates for a relatively faster crystallization rate. Therefore, the relatively constant and lower ΔT_c for the blends beyond 50 wt% PHB suggests a faster crystallization rate and thereby a reduced effect of interference in the co-crystallization at least for the now dominant PHB phase.

Besides, the onset temperature suggesting change in the nucleation driving force, the peak crystallization temperature gives practical information towards melt processing these blends. The maximum exothermal heat flow indicates for the temperature of most rapid crystallization. For specific processing conditions, this temperature is a reference point for annealing and acceleration of melt-stiffening.

These masterbatches of formulated PHBV compositions resulted in engineered immiscible blends with systematically well-defined trends in thermal properties. Solution rheology, and the melt and crystallization properties measured by DSC, suggested that the two phases interacted to influence, as well as to interfere with, the respective native blend component thermal properties – extent of crystallization and crystallization rate. It was therefore of interest to evaluate for an impact in the outcomes of microstructure developments, due to crystallization rate differences, on the bulk material thermo-mechanical properties (Section 3.3). Microstructural morphological differences were then studied by AFM (Section 3.4). Questions of an influence of blending on respective PHBV grade processibility were addressed with melt rheology measurements (Section 3.5).

3.3. *Blending of immiscible PHBV copolymers modulates resulting mechanical properties*

Mechanical properties from tensile testing revealed an influence of blend compositions with typical stress–strain curves shown in Fig. 6. The replicated results demonstrate a progressive significant transition with increasing PHB content from the more soft and ductile PHARIO PHBV, to the more stiff and brittle PHB (Fig. 7a, b, and c). PHB 0 wt% blend (i.e. 100 wt% PHARIO PHBV) exhibited elongation at break of at least 100% with the lowest Young's modulus (244 ± 100 MPa) and tensile strength (7 ± 2.5 MPa). These values are consistent with expectations for a pre-eutectic miscible PHBV reported in the literature [24,43]. On the other hand, the 100 wt% PHB gave the highest Young's modulus (1200 ± 75 MPa) and tensile strength (21.5 ± 1.1 MPa) with the lowest elongation at break (11.8 ± 5%) as also expected due to the more crystalline microstructure [18,44].

The stress–strain analysis was carried out using DMTA on film samples in a comparative analysis. PHBV/PHB blend samples with 75 and 100 wt% yielded suddenly, but they did not fracture catastrophically. It is difficult to speculate on the quality of fracture without additional replicates and post deepened evaluation of the broken samples. Such assessment was beyond the scope of the present investigation. The other samples with lower wt.% PHB yielded and stretched plastically to up to 100% strain at constant stress. The influence of blend composition on the quality of sample failure and fracture mechanisms will be important to evaluate and understand in the future and in the context of specific process conditions and application intent. The purpose of DMTA on these samples was to assess for an influence of blend composition on elastic modulus and yield strength. Outcomes of

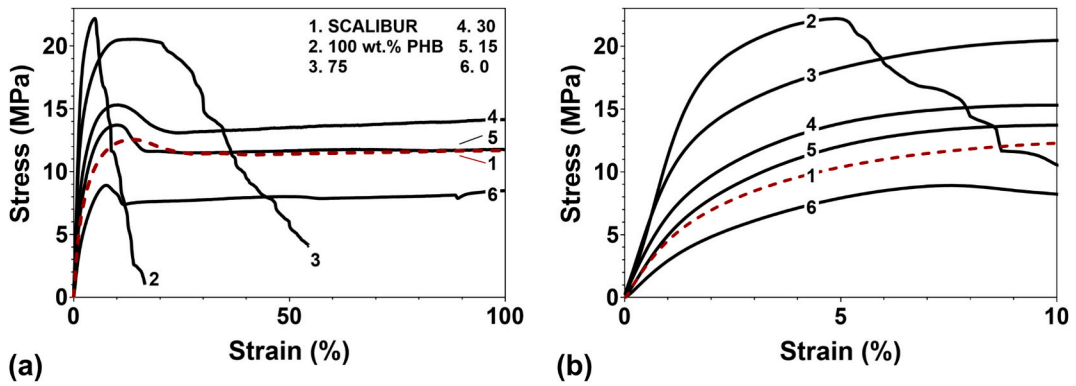

Fig. 6. (a) Typical stress–strain curves of PHB and PHARIO PHBV blends ranging from 0 to 100 wt% PHB (black lines) and SCALIBUR PHBV (red dashed line). (b) Zoomed in detail of the stress–strain curve up to 10% strain. Note that a strain of 100% was the maximum possible applied strain for these measurements.

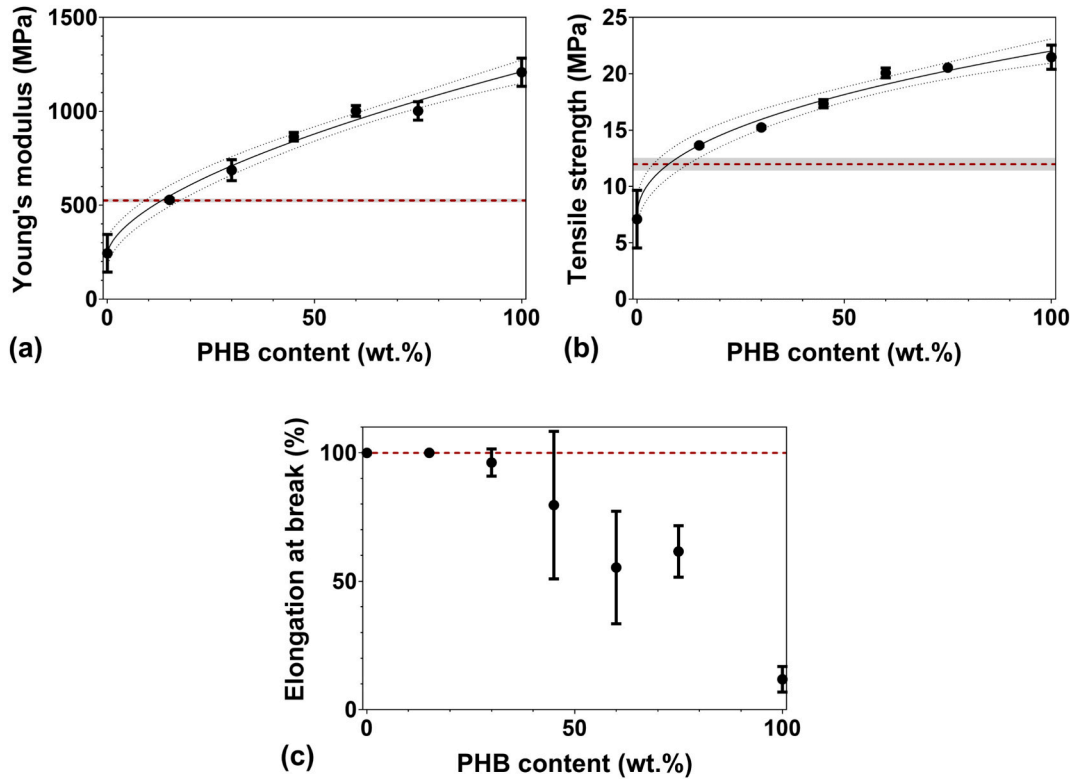

Fig. 7. Stress–strain results from mechanical testing (n = 2). Dependence of (a) Young's modulus, (b) maximum tensile strength, and (c) elongation at break on blend compositions (black dots). Properties of SCALIBUR PHBV shown by red dashed line. Shaded areas represent 95% confidence intervals. Note that a strain of 100% was the maximum possible measured strain for these evaluations.

mechanical properties, and specimen failure are to be developed in the ongoing research taking into account the application context and other factors like the type of test specimen and processing methods.

These outcomes from mechanical testing, at the extremes of 100 wt% PHARIO PHBV and 100 wt% PHB, well represent an expected range of the material behaviour as reported in the literature. Absolute differences in reported mechanical test results may arise for the same polymer due to differences in sample preparation, age, measurement conditions, and/or molecular weight [45]. For these blends, with all other factors being the same, as PHB content was increased, both Young's modulus and tensile strength increased in a well-defined trend from levels of PHARIO PHBV up to levels of PHB. However, the effect of PHB addition to the blend on the material elastic modulus and strength is most pronounced below 50 wt% PHB. Both these values increased markedly, by a factor of two, within 15 wt% PHB addition. In this regime of minor PHB added content, the blend melt and crystallization behaviour (Fig. 5) is most significantly influenced by the PHARIO PHBV, but there is also a progressive increase in the initial extent of crystallization (Fig. 5c). The more rapidly formed sites of crystalline regions within the microstructure may act as physical crosslinking elements that can contribute to resist applied stresses [46]. This effect would explain the increase in Young's modulus and tensile strength from the neat PHARIO PHBV mechanical properties. In contrast, beyond 50 wt% PHB, the increases in Young's modulus and tensile strength asymptotically approached the PHB levels, of 1071 ± 97 MPa and 21 ± 0.6 MPa, respectively. This development corresponds to the observed shift of the blend thermal properties (Fig. 5d). The DSC trends suggest microstructure crystallization rates that shift to being more strongly governed by PHB when it dominates in the weight fraction of the blend.

Fig. 7c shows elongation at break wherein the more ductile blends

(from 0 to 15 wt% PHB) will reach at least 100% elongation before failure. A decreasing trend with increasing PHB content was expected [20]. However, with less than 50 wt% PHB, the elongation at break can still exceed at least 60%. Even with minor amounts of added PHARIO PHBV, the elongation at break is suggested to become significantly greater than for the neat PHB. The less crystalline PHARIO PHBV enables the blend microstructure to undergo significantly more plastic deformation before facture, and this is attributed to a mobility of integrated deformable softer less-crystalline regions within the microstructure [47]. However, beyond 50 wt% PHB, the blends failed suddenly at the level of maximal tensile strength without extended plastic deformation. Reduced plastic deformation reflects a more crystalline microstructure (Fig. 5) imposing greater restriction for polymer chain mobility between crystallites. On the other hand, given the evident degree of plastic deformation before failure, some inherent level of compatibility must exist between the immiscible blends of PHB and PHARIO PHBV. This expectation is supported by the thermal analysis and solution rheology results (section 3.2). Interpenetration of polymer chains between interfaces of immiscible phases or crystallites, connecting the more and less crystalline regions, would allow a uniform transfer of stress across the material cross-section in tensile testing. This transfer mitigates risks for brittle fracture due to crack initiation and propagation between crystallites under loading, and it would lead to overall enhanced ductility and toughness [48,49].

Dynamic thermomechanical analysis (DMTA) was performed to assess elastic storage moduli as a function of temperature (Fig. 8a). All the blend grades exhibit a glassy-to-rubbery transition for the elastic storage modulus at a temperature ranging from 7 to 17 °C as a function of blend composition (Fig. 8b). The modulus decreases after the transition meaning that polymer blends become relatively more flexible above the transition temperature. The transition happens at a higher temperature compared to the glass transition temperature (Fig. 4b) as a distinction of a transition for the bulk crystallized microstructure versus the glass transition for an amorphous polymer blend microstructure formed after rapid quenching (−100 °C/min) and measured by DSC.

A plateau region of more stable elastic properties in the range of ambient temperature conditions was evident beyond the transition. However, the extent of this stability also varied as a function of the blend composition. Blends richer in PHARIO PHBV showed a shorter plateau temperature range and a sharper onset in softening with loss of storage modulus at relatively lower temperatures (Fig. 8b). PHB in the blend contributes to rigidity, and mechanic property stability over a wider temperature range. Therefore, blending less crystalline PHBV copolymers with a more crystalline PHBV provides a means to balance and compromise between property differences and requirements in applications with respect to strength and toughness, as well as in temperature sensitivity.

PHB 15 and 30 wt% blends, as well as the SCALIBUR PHBV, exhibited a transient hardening beyond the temperature dependent softening transition at above 100 °C. Such a transient rise and loss in the storage modulus as a function of temperature is also observed for PLA. It can be attributed to a cold crystallization process where the quenched-in amorphous structure gains sufficient mobility to allow for crystallization and thereby creates a transitional rise in the storage modulus [50–52]. Further heating leads to melting and a final collapse in the storage modulus suggesting a complete loss in the material microstructural integrity. The higher temperature transition may be indicative of the interactions at the interface between phases of more crystalline (hard domains) (Fig. 2a) embedded within the softer phase regions connected by interpenetrating polymer networks [53,54]. The SCALIBUR PHBV sample also revealed this higher temperature transition. Therefore, the blended PHB 30 wt% grade could reproduce the qualities of SCALIBUR PHBV. Target polymer quality and properties can be reproduced by solution blending of disparate types of PHBV into immiscible copolymer blends. This outcome supports the hypothesis that blending to create copolymer distributions for biphasic PHBV microstructures with more crystalline and less crystalline components is a means to engineer property specifications and one strategy in the downstream extraction process to achieve polymer production quality control.

3.4. *Respective blend component crystallization rates influence microstructures*

Assessments of differences in microstructures and resulting phase morphologies for the PHBV grades were made by AFM surface scans of the blend melt pressed discs (Fig. 2 and Fig. 9). Scans by AFM and peak force quantitative nanomechanical mapping (QNM) of stiffness values were acquired with replicate fields of view of 10 x10 μm^2. As also shown in Fig. 2 for PHARIO versus SCALIBUR PHBV, the AFM images of the formulated blends were similarly illustrative for tendencies and differences as a function of composition. Representative AFM images (Fig. 9, left) show outcomes of morphologies of QNM microstructure stiffness scaled respectively from hardest (light yellow) to softest (dark brown) zones. The corresponding distributions of stiffness (z_n) for each image are also plotted as a normalized frequency histogram (Fig. 9, right). The miscible copolymer blend (PHARIO PHBV) and the homopolymer (PHB) both exhibit single phase microstructures wherein the stiffness distribution was well-represented by a simple Gaussian distribution (Fig. 2 and Fig. 9). On the other hand, stiffness distributions of the blended PHBV grades were all better modelled by a Gaussian doublet peak, suggesting biphasic microstructures formed by immiscible blends (Fig. 9b). A peak doublet was most apparent for the scans on the discs made with PHBV grades of 15 and 30 wt% PHB. The stiffness maps for the 15 wt% PHB blend tended to be more of a dispersed biphasic microstructure morphology (Fig. 9a). The dispersed biphasic is characterized by spherical hard moieties. These may be interpreted as islands richer in more crystalline (PHB rich) zones, dispersed and embedded within a softer and less crystalline (PHARIO PHBV) host matrix. The

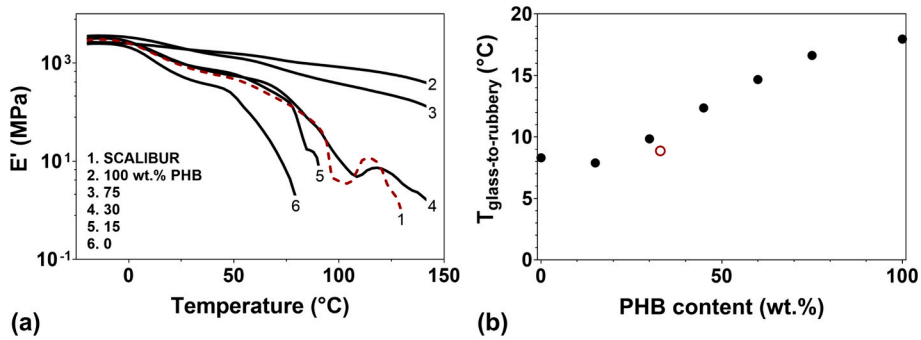

Fig. 8. (a) Elastic storage (E') of blend compositions (black lines) and SCALIBUR PHBV (red dashed line). (b) The peak temperature for the first derivative of elastic storage modulus in the temperature range of the glass-to-rubbery transition region. (black solid dots for blend compositions and red open dot for SCALIBUR PHBV with estimated PHB content described in section 3.2).

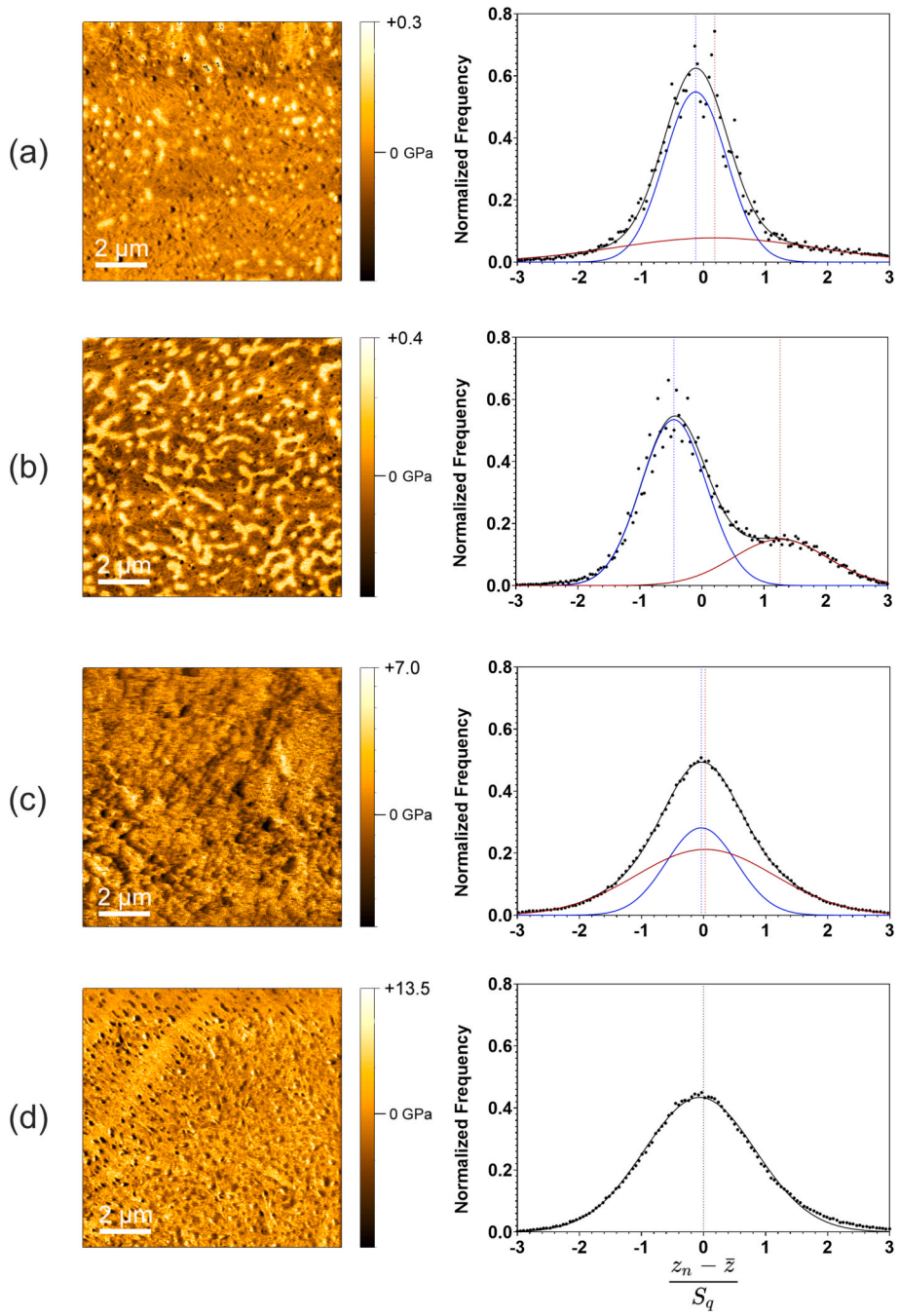

Fig. 9. PeakForce QNM stiffness maps (scan size 10 μm, left) and stiffness distribution-histogram plots (right) for (a) PHB 15 wt%, (b) PHB 30 wt%, (c) PHB 75 wt%, and (d) PHB 100 wt%. Trend lines for the distributions were fit to Gaussian (d), and Gaussian doublet (a, b, c) peak distributions (red and blue lines indicating individual peak locations) by non-linear least squares regression analysis.

AFM results for the PHBV grade with 30 wt% PHB most resembled SCALIBUR PHBV (Fig. 2a). In this case, the microstructure could be characterized as a layered-network biphasic morphology (Fig. 9b). The layered-network phase separated morphology consists of anisotropic and elongated harder domains intermingled within a softer matrix. Fig. 10 shows the likelihood of distribution and segregation representing the stiffness mapping. Notably, the interpreted outcomes are a collective microstructure development, resulting from the interaction, segregation, and co-crystallization of the polymers in the blend. Starting from the less crystalline extreme of the respective single-phase microstructures, a transition of microstructure morphologies can progress from a dispersed to a layered-network biphasic morphology depending on blend composition. The kind of biphasic microstructure that forms after cooling from the melt depends on crystallization onset, co-crystallization rates and extent of crystallinity developed as a function of the applied thermal history.

The trend in the AFM root mean square (rms) stiffness (Fig. 11) shows that the more crystalline PHB gives the highest rms stiffness (4.9 ± 3.0 GPa). In contrast, the as-produced PHBVs showed two distinct stiffness values depending on the feedstock used. The miscible and less crystalline PHARIO PHBV gives correspondingly the lowest stiffness of 0.09 ± 0.03 GPa. In contrast, the SCALIBUR PHBV, an immiscible blend with similar average 3HV content to the PHARIO PHBV, results in approximately a twofold higher stiffness (0.19 GPa). The immiscibility between interpreted more and less crystalline phase fractions introduces an apparent reinforcing effect. Interestingly, this effect is replicated

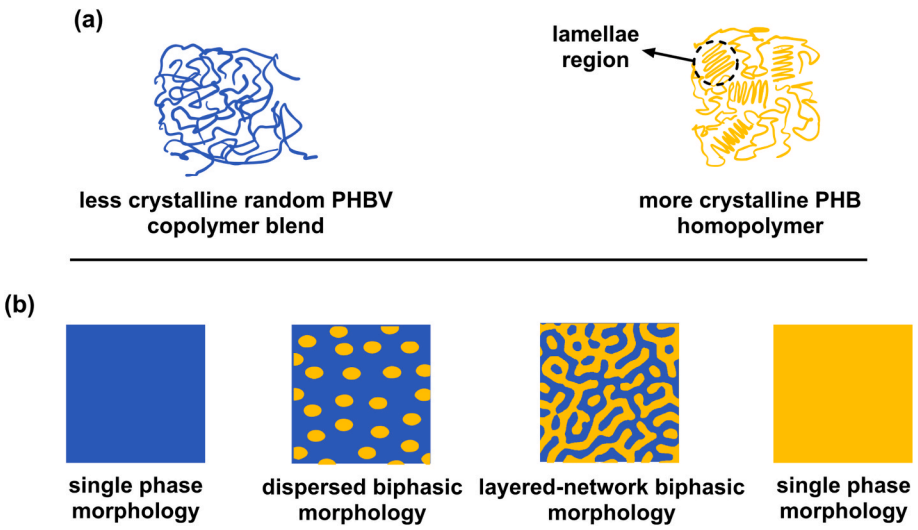

Fig. 10. (a) Schematic representation of entangled polymer chain model of less crystalline PHBV (right, shown in blue), and folded chains or lamellae structures embedded in disordered chains in more crystalline PHB homopolymer (right, shown in yellow); (b) Schematic representation microstructure phases morphologies: single uniform phase morphology exhibited by the neat PHAs (left: PHBV, right: PHB)), and the resulting dispersed biphasic morphology (middle left) and layered-network biphasic morphology (middle right) for the PHBV/PHB immiscible blends.

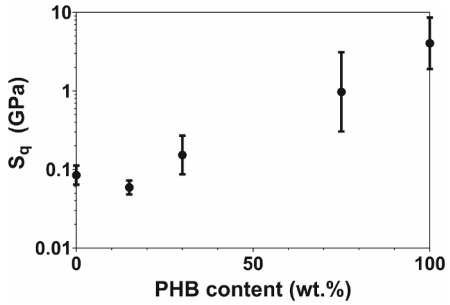

Fig. 11. The trend of increasing average rms stiffness (n = 3) as a function of increasing PHB wt.% in blends with PHARIO PHBV. Higher fractions of the PHB homopolymer result in PHBV grades with greater rms stiffness.

progressively due to the blending of PHB with PHARIO PHBV, as a progressive increase in rms stiffness correlates with added wt.% PHB. Notably, the 30 wt% PHB blend gave a comparable rms stiffness value to that of the as-extracted SCALIBUR PHBV, and this similarity was expected based on the estimation of the effective weight of PHB in SCALIBUR PHBV (Section 3.2). Details such as size, shape, and distribution of the harder phase domains embedded in the softer microstructure matrix may be expected to contribute to the thermomechanical and rheological properties of such immiscible PHBV copolymer blend grades. The microstructure will be dependent on factors including but not limited to processing methods, respective domain/component 3HV contents (extent of crystallinity and crystallization rate), as well as the average molecular weight and distribution of the blend components. Even if the discs produced for AFM evaluations were distinct in thermal history from the films produced for mechanical testing, analogous results were obtained, and this suggests inherent properties for the blends. Both sets of results were further supported by trends and expectations that could be derived from DSC measurements. Therefore, general features and expectations for properties of immiscible PHBV copolymer blends may be, in the first instance, understood and characterized from different kinds of assessment approaches with DSC as a first quicker step of blend property scanning.

PHAs can be dissolved (and thereby extracted) in many non-halogenated solvents at elevated temperatures including but not limited to alcohols, ketones and carbonates [31,40,55]. In this manner, a blend of homo and/or copolymers are mixed homogenously. The quality of the microstructure and morphology of the phase separation for immiscible blends will be influenced by the conditions under which crystallization takes place – in solution processing wherein potential for gelation is also a factor [56], and with subsequent melt processing if applicable. Temperatures and kinetics of gelation are both PHA grade and solvent dependent [31]. Therefore, context of the solvent-polymer selection and the processing objectives are important for selecting solution process conditions. In general, processing conditions with or without solvents are expected to influence microstructural morphological outcomes of co-crystallization and relative crystallization rates of the components for a melted or dissolved (immiscible) copolymer blend. For example, melt enthalpy peaks can be distinct between solution cast and melt quenched microstructures for the same homopolymer, copolymer, or copolymer blend [56].

The AFM analysis, together with mechanical testing, suggests that PHBV quality and properties can be systematically engineered by the scalable methods of solution blending. Solution blending is intrinsic to methods of PHBV recovery using green solvents. It was unexpected to find that a key to achieving enhanced PHBV properties was by blending immiscible PHBV co-polymers. Optimization of properties by blending to fine-tune specific needs in thermo-mechanical properties can be made according to the demands and context of specific applications of interest, case-by-case. Applications for PHAs often require melt processing of the polymers. Therefore, an assessment of blend influence on PHBV grade processability was evaluated using melt rheology.

3.5. *Blend grade and differences in processability from melt rheology*

Characterization of the polymer pseudoplasticity, i.e. shear-thinning non-Newtonian behaviour, and polymer melt hardening/crystallization rates is central to designing optimal polymer processing conditions. The influence of the blend compositional changes on shear thinning melt flow (pseudoplastic) behaviour, and the subsequent crystallization-induced stiffening rates due to cooling was analysed. A typical measurement in three segments at constant 2% strain (1 – isothermal time sweep (1 Hz, 195 °C), 2 – isothermal frequency sweep (1 to 1000 Hz, 195 °C), and 3 – quench time sweep (1 Hz, 195 to 15 °C)) is shown in Fig. S2.

Fig. 12a illustrates the complex viscosity (η*) determined at the end of isothermal sweep [40]. Typically, melt viscosity projected to zero

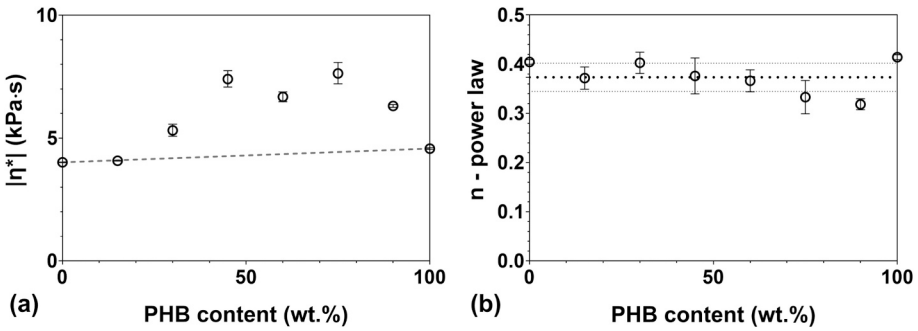

Fig. 12. PHBV blend pseudoplastic melt flow behaviour and characterization. Summary of (a) isothermal complex viscosity (η*) at 195 °C and (b) the power law index with overall mean and 95% CI (dotted lines) as a function of PHBV blend grades from 0 to 100 wt% PHB.

shear rate can be related to weight average molecular weight (M_w) by the classical Mark-Houwink-Sakurada relationship [57,58]. Under conditions of constant shear rate and temperature, M_w is also reported to scale linearly with η* [59]:

$$M_w = a \cdot \eta^*_{(T,f)} + b \tag{4}$$

where the 'a' and 'b' constants are dependent on the type of PHA. In previous work [38], miscible copolymer blends of PHBV (0 to 50 average wt.% 3HV) gave a common average trend, and the same constants were applicable independent of the miscible blend co-monomer composition (Fig. S3). Except for the 0 and 100 wt% PHB blends, the blended PHBV grades in the present study are all immiscible. Fig. 12a shows a positive deviation from the linear trend (dashed line) that would have been expected based on the previous experience (Fig. S3). This deviation can be attributed to interactions between the interfaces of immiscible domains in the melt [60,61]. This interpretation supports the idea of interacting and/or interpenetrating phases in the microstructure as also indicated from outcomes of mechanical testing and AFM (Fig. 7 and Fig. 9), DSC measurements (Fig. 5), and solution rheology (Fig. 4a). Specifically, the presence of 3-hydroxyvalerate (3HV) side groups introduces steric hindrance that resists chain mobility during deformation. This structural effect increases intermolecular interactions and may contribute to the observed complex viscosity response of the blends. Therefore, both molecular weight and immiscible blend composition play decisive roles in governing the rheological behaviour of these immiscible grades of PHBV. The implication is for necessary tuning of processing (shear stress and directionality) and for influencing domain morphology (size, distribution, and directionality) to affect the final material properties [62]. The influence of processing conditions on properties for immiscible PHBV blends forms part of the ongoing investigations.

Pseudoplastic behaviour, also known as shear thinning, is central to polymer processing because it governs how a melted polymer flows as a function of applied shear rates. The extent to which viscosity decreases as shear rates increase (segment 2, Fig. S2) is a key aspect impacting common thermoplastic polymer melt processing methods like extrusion, moulding, injection moulding, and fibre spinning [63–65]. Understanding and controlling pseudoplasticity is part of optimization for melt processing, and for achieving controlled and targeted final product property specifications. Different shear thinning responses can mean that different processing operating conditions may be required. Therefore, it was of interest to evaluate if the different immiscible blend grades, from 100 wt% PHARIO PHBV to 100 wt% PHB, exhibited similar or different shear thinning behaviour.

Pseudoplastic melt flow behaviour may be modelled using the Cross model or the simplified Power-law models [66,67]. These models depict flow behaviour of a polymer melt during processing. The blend PHBV grade melt flow behaviour was characterized with the Power-law model in the linear range of the measured trend at higher angular frequencies [68]:

$$|\eta^*| \sim k \cdot \gamma^{(n-1)} \tag{5}$$

where $|\eta^*|$ is the complex viscosity (Pa·s), n is the Power-law (shear thinning) index, k is material consistency index (Pa-s), and γ is the angular frequency (rad/s). Polymer melts will typically exhibit n values in the range of 0.2 – 0.6 [69]. It is a property of the type and chemical structure of a given polymer or polymer blend [62]. n is equal to 1 for Newtonian fluids wherein there is no influence of shear deformation rate on the viscosity.

Fig. 12b summarizes the observation of the Power-law index as a function of the PHBV blend composition. The obtained Power-law index (ranging from 0.31 to 0.39) for the PHB/PHBV blends showed no noticeable dependence on blend composition. This indicated that, in the molten state, the viscosity of PHB/PHBV blends exhibited a similar shear-rate dependence during polymer melt processing. In contrast, the PHB/PHBV blend composition has a pronounced influence on the onset temperature of melt crystallization (Fig. 5), which directly affects melt-stiffening behaviour. This crystallization-induced stiffening, in turn, will determine the suitability of the biopolymer for specific processing techniques, such as injection moulding, cast sheet extrusion, and blow moulding. Furthermore, the melt crystallization onset temperature governs the achievable fabrication rates and throughput capacities during polymer product manufacturing.

Blend composition influences crystallization-induced stiffening rate and its temperature range when cooling from the melt (Fig. 13). PHB 0 wt% (i.e. PHARIO PHBV) exhibited a gradual steady but still relatively slow progressive increase in complex viscosity during cooling. Even though PHARIO PHBV will crystallize to a low but measurable crystallinity over hours and days [24], the relative lack of crystallization-induced stiffening is evident from Fig. 13a. PHBVs have been advocated in the literature due to an interest to increase the processing window and avoid brittle materials compared to the homopolymer PHB [18]. However, the downside of the less crystalline PHBVs is the slow crystallization rate, making these co-polymers more difficult to process. Moulding cycle times in melt production runs would need to be longer, making articles time-consuming and expensive to manufacture [63].

By the incorporation of even a minor fraction of a more crystalline component (15 to 60 wt% PHB), crystallization-induced stiffening rates are improved significantly upon cooling. Subject to the weight fraction of PHB added to the blend, a progressively more rapid stiffening (storage modulus increase) was observed during the cooling segment between 140 and 56 °C, likely due to a faster crystallization of the harder domain (Fig. 9). The peak and onset of crystallization-induced stiffening temperatures were determined from the dG'/dT trend (Fig. S4). Fig. 13b therefore illustrates, by example, how grades of immiscible PHBV blends can be systematically tuned to significantly influence peak crystallization-induced stiffening temperatures and rates. The observed narrow range of peak temperature for stiffening (storage modulus increase) (Fig. 13b) may be due to non-isothermal physical crosslinking

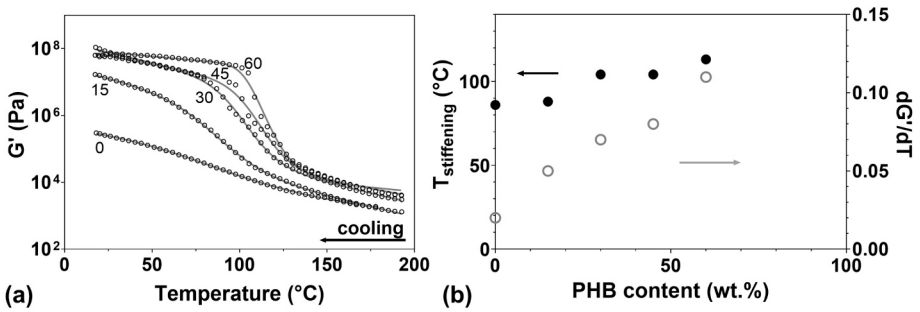

Fig. 13. (a) The segmental increase in melt shear storage modulus (G') of the PHBV grades during cooling (from 195 to 15 °C at −14.4 °C/min) with wt. % PHB as indicated by number in the figure. (b) An influence of the PHBV blend composition (wt. % PHB as indicated) on the peak temperature ($T_{stiffening}$) and rate of the crystallization-induced stiffening process (dG'/dT) is indicated by the slope of the change in modulus as a function of temperature.

processes that result in elasticity developments within the polymer melt due to the more crystalline component. The cooling rate in processing is expected to also influence developments of properties due to temperature sensitivity of crystal nucleation and nuclei growth rates. This brings an additional degree of freedom to influence the development of domain size and morphology in such interpenetrating biphasic microstructures. How processing conditions can be systematically applied to influence the distribution and scale of observed dispersed and/or layered-network biphasic microstructures (Fig. 9), and thereby tune mechanical properties, is an opportunity that requires further investigation that was beyond the scope of the present work. Formulating PHBV copolymer blend distributions enables parameters to be adjusted for processing and production efficiency as well as for tuning the final article mechanical property specifications (section 3.3).

Polymer grade melt rheology analysis, including melt flow and stiffening rates during cooling, informs decisions for selecting suitable processing operating parameters. Such parameters may need to be tailored, case-by-case, for a range of possible immiscible PHA blend types, to ensure consistently robust optimal processing and final article application performances. PHA melt extrusion parameters (i.e. barrel/die temperature, screw speed, extrudate cooling draw-off speed, etc.) can be initially established heuristically and linked to respective assessments of blend thermal and rheological properties like melting temperature, melt rheology, and the crystallization-induced stiffening behaviour. Categorically matched thermal and melt rheology behaviour can in this way help to facilitate rapid on-site batch-to-batch quality control and make deterministic process operating adjustments from assessment of grab samples before production runs.

The phenomena of integration and co-crystallization of the PHBV copolymer from PHB to PHV was extensively reviewed by Laycock et al [18] and further evaluated in a deepened investigation of these blends and blend fractions [26]. The present investigation brings forward an opportunity to systematically manipulate the polymer properties and to adjust the product quality by the formulation of specifically *immiscible* copolymer blends during or after the biological process. Evidence of co-crystallization modulation in the present work is suggested by the influence of blending PHB in PHBV (0 to 50% wt. PHB), and PHBV into PHB (50 to 100% wt. PHB), due to the interplay of the blend components on measured properties, such as in solution rheology (Fig. 4), and the outcomes of thermal properties by DSC (Fig. 5). This interplay of the blend composition together with the processing methods will influence the microstructure morphology and properties such as crystallization-induced stiffening (Fig. 13), and mechanical properties – strength, yield and elongation at break (Fig. 7). These effects are interpreted as the combination of co-crystallization, and the inherent partial compatibility between the two distinct phase domains. Together with the interfacial phase interpenetration and the phase interactions under stress and strain due to the inherently compatibilized networked 'hard' and 'soft' phases, a balance of strength and toughness is imparted to these biphasic microstructures.

4. Conclusion

Solution blending of poly(3-hydroxybutyrate-*co*-3-hydroxyvalerate) copolymers, that are sufficiently distinct in respective intrinsic extent of crystallinity and crystallization rate, will result in PHBV grades of immiscible copolymer blends. Such blends can result in biphasic microstructures depicted by dispersed and layered-network hard and soft phase morphologies. These phases will develop due to the combination of partial miscibility (inherent compatibility) of the blend components driving interactions and interferences that can ensue during processing and crystallization processes. The biphasic PHBV grades produced in the current work enabled a demonstration of systematic tuning of melt stiffening and the potential to steer mechanical properties for strength and ductility. Judiciously tuned immiscible PHBV blend compositions, in this study the 15–30 wt% PHB range in a pre-eutectic PHBV, exhibit analogous thermoplastic elastomer-like behaviour, with flexibility like elastomeric materials and yet being processable using conventional thermoplastic equipment. Furthermore, this composition range matched properties of the SCALIBUR PHBV that was independently recovered from a PHA-rich biomass by non-halogenated solvent extraction methods. Therefore, it is anticipated that solution blending methods can be readily and efficiently integrated into methods of PHBV extraction and recovery at industrial scale as part of tailoring properties for industrial applications and for masterbatch production quality control. The results support that immiscible PHBV blends, and their processing, are important to understand and develop further in continued PHA research for PHBV supply chains that enable industrial applications.

CRediT authorship contribution statement

Sanjay Pal: Writing – review & editing, Writing – original draft, Visualization, Validation, Supervision, Methodology, Investigation, Formal analysis, Data curation, Conceptualization. **Liang-Shin Wang:** Writing – review & editing, Writing – original draft, Visualization, Validation, Supervision, Methodology, Investigation, Formal analysis, Data curation, Conceptualization. **Ana Jiménez Vergel:** Investigation. **Philip Kridiotis:** Investigation. **Zandrie Borneman:** Writing – review & editing, Supervision. **Kitty Nijmeijer:** Writing – review & editing, Supervision. **Alan Werker:** Writing – review & editing, Supervision, Software, Methodology, Conceptualization.

Declaration of competing interest

The authors declare that they have no known competing financial interests or personal relationships that could have appeared to influence the work reported in this paper.

Acknowledgment

This work was performed in the cooperation framework of Wetsus,

European Centre of Excellence for Sustainable Water Technology (www.wetsus.nl). Wetsus is co-funded by European Union programmes (Horizon Europe, LIFE, Interreg and EDRF), the Province of Fryslân and the Dutch Government: Ministry of Economic Affairs (TTT, SBO & PPS-I/TKI Water Technology), Ministry of Education, Culture and Science (TTT & SBO) and Ministry of Infrastructure and Water Management (National Growth Fund - UPPWATER). The authors like to thank the participants of the research theme "Biopolymers from water" for the fruitful discussions and their financial support - Paques Biomaterials BV, STOWA, SNB, and Unilever. This research was co-founded by the Agro2Curcular project (agro2circular.eu) approved by the European Union's Horizon 2020 research and innovation programme under grant agreement No. 101036838, and Wetsus-TU Eindhoven academic cooperation. The work has benefited from the support and dedication of the Wetsus administration staff and technical support teams. Authors acknowledge and thank the two reviewers for many good and detailed supportive comments and suggestions in the revision process.

Appendix A. Supplementary data

Supplementary data to this article can be found online at https://doi.org/10.1016/j.eurpolymj.2026.114676.

Data availability

Data will be made available on request.

References

[1] Bauchmüller Verena, Carus Michael, Chinthapalli Raj, Dammer Lara, Hark Nicolas, Partanen Asta, Ruiz Pauline, Lajewski Silvia, BioSinn Products for which biodegradation makes sense, (2021). www.renewable-carbon.eu/publications.
[2] L. Ahmadi, J. Shadbahr, G.W. Shim, M. Hawco, Review of the global evolution of regulations on single-use plastics and lessons drawn for Canada, Waste Manage. Res. (2023), https://doi.org/10.1177/0734242X231184451.
[3] A. Pandey, N. Adama, K. Adjallé, J.F. Blais, Sustainable applications of polyhydroxyalkanoates in various fields: a critical review, Int. J. Biol. Macromol. 221 (2022) 1184–1201, https://doi.org/10.1016/j.ijbiomac.2022.09.098.
[4] P. Kehrein, M. van Loosdrecht, P. Osseweijer, M. Garfí, J. Dewulf, J. Posada, A critical review of resource recovery from municipal wastewater treatment plants – market supply potentials, technologies and bottlenecks, Environ. Sci. (Camb) 6 (2020) 877–910, https://doi.org/10.1039/C9EW00905A.
[5] M. Koller, The handbook of polyhydroxyalkanoates, in: The Handbook of Polyhydroxyalkanoates, 2020, https://doi.org/10.1201/9780429296635/HANDBOOK-POLYHYDROXYALKANOATES-MARTIN-KOLLER.
[6] Á. Estévez-Alonso, R. Pei, M.C.M. van Loosdrecht, R. Kleerebezem, A. Werker, Scaling-up microbial community-based polyhydroxyalkanoate production: status and challenges, Bioresour. Technol. 327 (2021), https://doi.org/10.1016/J.BIORTECH.2021.124790/SCALING_UP_MICROBIAL_COMMUNITY_BASED_POLYHYDROXYALKANOATE_PRODUCTION_STATUS_AND_CHALLENGES.PDF.
[7] R. Pei, E. de Vries, A. Estévez, J. Sousa, H. Dijkman, J. Tamis, A. Werker, Demonstrating performance in scaled-up production and quality control of polyhydroxyalkanoates using municipal waste activated sludge, Water Res. 275 (2025) 123160, https://doi.org/10.1016/J.WATRES.2025.123160.
[8] G. Pagliano, P. Galletti, C. Samorì, A. Zaghini, C. Torri, Recovery of polyhydroxyalkanoates from single and mixed microbial cultures: a review, Front. Bioeng. Biotechnol. 9 (2021) 624021, https://doi.org/10.3389/FBIOE.2021.624021/BIBTEX.
[9] L. Ahmadi, J. Shadbahr, G.W. Shim, M. Hawco, Review of the global evolution of regulations on single-use plastics and lessons drawn for Canada, Waste Manage. Res. (2023), https://doi.org/10.1177/0734242X231184451.
[10] G. Mannina, D. Presti, G. Montiel-Jarillo, J. Carrera, M.E. Suárez-Ojeda, Recovery of polyhydroxyalkanoates (PHAs) from wastewater: a review, Bioresour. Technol. (2019) 122478, https://doi.org/10.1016/j.biortech.2019.122478.
[11] P.C. Sabapathy, S. Devaraj, K. Meixner, P. Anburajan, P. Kathirvel, Y. Ravikumar, H.M. Zabed, X. Qi, Recent developments in Polyhydroxyalkanoates (PHAs) production - a review, Bioresour. Technol. 306 (2020) 123132, https://doi.org/10.1016/j.biortech.2020.123132.
[12] O.M. Janarthanan, B. Laycock, L. Montano-Herrera, Y. Lu, M.V. Arcos-Hernandez, A. Werker, S. Pratt, Fluxes in PHA-storing microbial communities during enrichment and biopolymer accumulation processes, N. Biotechnol. 33 (2016) 61–72, https://doi.org/10.1016/J.NBT.2015.07.007.
[13] M. Koller, A. Mukherjee, Polyhydroxyalkanoates – production, properties, and biodegradation, in: Biodegradable Polymers in the Circular Plastics Economy, Wiley, 2022, pp. 145–204, https://doi.org/10.1002/9783527827589.ch6.
[14] M. Villano, M. Beccari, D. Dionisi, S. Lampis, A. Miccheli, G. Vallini, M. Majone, Effect of pH on the production of bacterial polyhydroxyalkanoates by mixed cultures enriched under periodic feeding, Process Biochem. 45 (2010) 714–723, https://doi.org/10.1016/J.PROCBIO.2010.01.008.
[15] G. De Grazia, L. Quadri, M. Majone, F. Morgan-Sagastume, A. Werker, Influence of temperature on mixed microbial culture polyhydroxyalkanoate production while treating a starch industry wastewater, J. Environ. Chem. Eng. 5 (2017) 5067–5075, https://doi.org/10.1016/J.JECE.2017.09.041.
[16] F. Valentino, F. Morgan-Sagastume, S. Campanari, M. Villano, A. Werker, M. Majone, Carbon recovery from wastewater through bioconversion into biodegradable polymers, N. Biotechnol. 37 (2017) 9–23, https://doi.org/10.1016/J.NBT.2016.05.007.
[17] B. Laycock, M.V. Arcos-Hernandez, A. Langford, J. Buchanan, P.J. Halley, A. Werker, P.A. Lant, S. Pratt, Thermal properties and crystallization behavior of fractionated blocky and random polyhydroxyalkanoate copolymers from mixed microbial cultures, J. Appl. Polym. Sci. 131 (2014), https://doi.org/10.1002/app.40836.
[18] B. Laycock, P. Halley, S. Pratt, A. Werker, P. Lant, The chemomechanical properties of microbial polyhydroxyalkanoates, Prog. Polym. Sci. 38 (2013) 536–583, https://doi.org/10.1016/J.PROGPOLYMSCI.2012.06.003.
[19] K. Molenveld, W. Post, S.F. Ferreira, G. de Sévaux, M. Hartstra, Paving the way for biobased materials, 2022. https://research.wur.nl/en/publications/paving-the-way-for-biobased-materials-a-roadmap-for-the-market-in.
[20] A. Werker, S. Bengtsson, P. Johansson, P. Magnusson, E. Gustafsson, M. Hjort, S. Anterrieu, L. Karabegovic, T. Alexandersson, A. Karlsson, F. Morgan-Sagastume, L. Sijstermans, M. Tietema, E. Wypkema, Y. van der Kooij, A. Deeke, C. Uijterlinde, L. Korving, Y. van der Kooij, A. Deeke, C. Uijterlinde, L. Korving, Production quality control of mixed culture poly(3-hydroxbutyrate-co-3-hydroxyvalerate) blends using full-scale municipal activated sludge and non-chlorinated solvent extraction, in: M. Koller (Ed.), The Handbook of Polyhydroxyalkanoates: Kinetics, Bioengineering, and Industrial Aspects, 1st ed., CRC Press, 2020, p. 58, https://doi.org/https://doi.org/10.1201/9780429296635.
[21] A. Cao, K.I. Kasuya, H. Abe, Y. Doi, Y. Inoue, Studies on comonomer compositional distribution of the bacterial poly(3-hydroxybutyric acid-co-3-hydroxypropionic acid)s and crystal and thermal characteristics of their fractionated component copolyesters, Polymer (guildf). 39 (1998) 4801–4816, https://doi.org/10.1016/S0032-3861(97)10146-X.
[22] Y. Wang, S. Yamada, N. Asakawa, T. Yamane, N. Yoshie, Y. Inoue, Comonomer compositional distribution and thermal and morphological characteristics of bacterial poly(3-hydroxybutyrate-co-3-hydroxyvalerate)s with high 3-hydroxyvalerate content, Biomacromolecules 2 (2001) 1315–1323, https://doi.org/10.1021/bm010128o.
[23] B. Laycock, M.V. Arcos-Hernandez, A. Langford, S. Pratt, A. Werker, P.J. Halley, P. A. Lant, Crystallisation and fractionation of selected polyhydroxyalkanoates produced from mixed cultures, N. Biotechnol 31 (2014) 345–356, https://doi.org/10.1016/J.NBT.2013.05.005.
[24] S. Bengtsson, A. Werker, C. Visser, L. Korving, PHARIO stepping stone to a sustanable value chain for PHA bioplastics using municipal activated sludge, STOWA (2017).
[25] M.V. Arcos-Hernández, B. Laycock, B.C. Donose, S. Pratt, P. Halley, S. Al-Luaibi, A. Werker, P.A. Lant, Physicochemical and mechanical properties of mixed culture polyhydroxyalkanoate (PHBV), Eur. Polym. J. 49 (2013) 904–913, https://doi.org/10.1016/J.EURPOLYMJ.2012.10.025.
[26] A. Langford, C.M. Chan, S. Pratt, C.J. Garvey, B. Laycock, The morphology of crystallisation of PHBV/PHBV copolymer blends, Eur. Polym. J. 112 (2019) 104–119, https://doi.org/10.1016/J.EURPOLYMJ.2018.12.022.
[27] S.J. Organ, P.J. Barham, Phase separation in a blend of poly(hydroxybutyrate) with poly(hydroxybutyrate-co-hydroxyvalerate), Polymer (Guildf). 34 (1993) 459–467, https://doi.org/10.1016/0032-3861(93)90535-I.
[28] S.J. Organ, Phase separation in blends of poly(hydroxybutyrate) with poly (hydroxybutyrate-co-hydroxyvalerate): variation with blend components, 1994.
[29] N. Yoshie, M. Saito, Y. Inoue, Effect of chemical compositional distribution on solid-state structures and properties of poly(3-hydroxybutyrate-co-3-hydroxyvalerate), Polymer (Guildf). 45 (2004) 1903–1911, https://doi.org/10.1016/J.POLYMER.2004.01.025.
[30] A.G. Werker, P. Johansson, P. Magnusson, Process for the extraction of polyhydroxyalkanoates from biomass, EP 2 956 493 B1, 2023.
[31] A. Werker, R. Pei, K. Kim, G. Moretto, A. Estevez-Alonso, C. Vermeer, M. Arcos-Hernandez, J. Dijkstra, E. de Vries, Thermal pre-processing before extraction of polyhydroxyalkanoates for molecular weight quality control, Polym. Degrad. Stab. 209 (2023) 110277, https://doi.org/10.1016/J.POLYMDEGRADSTAB.2023.110277.
[32] O.F. Solomon, I.Z. Ciută, Détermination de la viscosité intrinsèque de solutions de polymères par une simple détermination de la viscosité, J. Appl. Polym. Sci. 6 (1962) 683–686, https://doi.org/10.1002/APP.1962.070062414.
[33] Document Revision History: PeakForce QNM User Guide User Guide, (2011).
[34] M. Scandola, G. Ceccorulli, M. Pizzoli, M. Gazzano, Study of the crystal phase and crystallization rate of bacterial poly(3-hydroxybutyrate-co-3-hydroxyvalerate), Macromolecules 25 (1992) 1405–1410, https://doi.org/10.1021/ma00031a008.
[35] Scalibur – Leading A Revolution In Biowaste Recycling, (n.d.). https://scalibur.eu/ (accessed January 3, 2024).
[36] G. Odian, Principles of Polymerization, Wiley, 2004, 10.1002/047147875X.
[37] S. Kéki, M. Zsuga, Á. Kuki, Theoretical size distribution in linear step-growth polymerization for a small number of reacting species, J. Phys. Chem. B 117 (2013) 4151–4155, https://doi.org/10.1021/jp401238m.
[38] C.M. Chan, P. Johansson, P. Magnusson, L.J. Vandi, M. Arcos-Hernandez, P. Halley, B. Laycock, S. Pratt, A. Werker, Mixed culture polyhydroxyalkanoate-rich biomass assessment and quality control using thermogravimetric

measurement methods, Polym. Degrad. Stab. 144 (2017) 110–120, https://doi.org/10.1016/J.POLYMDEGRADSTAB.2017.07.029.
[39] T.G. Fox, P.J. Flory, Second-order transition temperatures and related properties of polystyrene. I. Influence of molecular weight, J. Appl. Phys. 21 (1950) 581–591, https://doi.org/10.1063/1.1699711.
[40] S. Pal, P. Kridiotis, A. Jiménez Vergel, Z. Medved, R. Barbosa, A. Werker, Direct melt extrusion of polyhydroxyalkanoate solvent-rich gels after polymer extraction and melt processing with integrated solvent recovery, J. Clean. Prod. 517 (2025) 145818, https://doi.org/10.1016/J.JCLEPRO.2025.145818.
[41] B.A. Wolf, Intrinsic viscosities of polymer blends and polymer compatibility: self-organization and flory–huggins interaction parameters, Macromol. Chem. Phys. 219 (2018), https://doi.org/10.1002/macp.201800249.
[42] G. Groeninckx, C. Harrats, M. Vanneste, V. Everaert, Crystallization, micro- and nano-structure, and melting behavior of polymer blends, in: Polymer Blends Handbook, Springer, Netherlands, Dordrecht, 2014, pp. 291–446, https://doi.org/10.1007/978-94-007-6064-6_5.
[43] S. Alfano, E. Doineau, C. Perdrier, L. Preziosi-Belloy, N. Gontard, A. Martinelli, E. Grousseau, H. Angellier-Coussy, Influence of the 3-hydroxyvalerate content on the processability, nucleating and blending ability of poly(3-hydroxybutyrate-co-3-hydroxyvalerate)-based materials, ACS Omega 9 (2024) 29360–29371, https://doi.org/10.1021/ACSOMEGA.4C01282/SUPPL_FILE/AO4C01282_SI_001.PDF.
[44] S. Khanna, A.K. Srivastava, Recent advances in microbial polyhydroxyalkanoates, Process Biochem. 40 (2005) 607–619, https://doi.org/10.1016/J.PROCBIO.2004.01.053.
[45] K. Wang, A.A. Abdala, N. Hilal, M.K. Khraisheh, Mechanical characterization of membranes, in: Membrane Characterization, Elsevier, 2017, pp. 259–306, https://doi.org/10.1016/B978-0-444-63776-5.00013-9.
[46] T.R. Anju, J. Sindhu Rachel, Biopolymer-based interpenetrating polymer networks, in: Handbook of Biopolymers, Springer Nature, Singapore, Singapore, 2023, pp. 435–467, https://doi.org/10.1007/978-981-19-0710-4_16.
[47] S.F. Xavier, Properties and performance of polymer blends, in: Polymer Blends Handbook, Springer Netherlands, Dordrecht, 2014, pp. 1031–1201, https://doi.org/10.1007/978-94-007-6064-6_12.
[48] V. Bouchart, N. Bhatnagar, M. Brieu, A.K. Ghosh, D. Kondo, Study of EPDM/PP polymeric blends: mechanical behavior and effects of compatibilization, Comptes Rendus Mécanique 336 (2008) 714–721, https://doi.org/10.1016/J.CRME.2008.06.004.
[49] A.R. Ajitha, S. Thomas, Introduction: Polymer blends, thermodynamics, miscibility, phase separation, and compatibilization, Compatib. Polymer Blends (2020) 1–29, https://doi.org/10.1016/B978-0-12-816006-0.00001-3.
[50] S. Yang, Z.-H. Wu, W. Yang, M.-B. Yang, Thermal and mechanical properties of chemical crosslinked polylactide (PLA), Polym. Test. 27 (2008) 957–963, https://doi.org/10.1016/j.polymertesting.2008.08.009.
[51] J.D. Badia, E. Strömberg, S. Karlsson, A. Ribes-Greus, Material valorisation of amorphous polylactide. Influence of thermo-mechanical degradation on the morphology, segmental dynamics, thermal and mechanical performance, Polym. Degrad. Stab. 97 (2012) 670–678, https://doi.org/10.1016/j.polymdegradstab.2011.12.019.
[52] M. Cristea, D. Ionita, M.M. Iftime, Dynamic mechanical analysis investigations of PLA-based renewable materials: how are they useful? Materials 13 (2020) 5302, https://doi.org/10.3390/MA13225302.
[53] D.A. Thomas, L.H. Sperling, Interpenetrating polymer networks, Polym. Blends (1978) 1–33, https://doi.org/10.1016/B978-0-12-546802-2.50007-5.
[54] T.R. Anju, J.S. Rachel, Biopolymer-based interpenetrating polymer networks, Handbk. Biopolym. (2023) 435–467, https://doi.org/10.1007/978-981-19-0710-4_16.
[55] C.M. Vermeer, M. Nielsen, V. Eckhardt, M. Hortensius, J. Tamis, S.J. Picken, G.M. H. Meesters, R. Kleerebezem, Systematic solvent screening and selection for polyhydroxyalkanoates (PHBV) recovery from biomass, J. Environ. Chem. Eng. 10 (2022), https://doi.org/10.1016/j.jece.2022.108573.
[56] L. Wang, A. Werker, K. Nijmeijer, Z. Borneman, Toward sustainable membrane fabrication using poly(3-hydroxybutyrate-co-3-hydroxyvalerate) copolymer blends and non-halogenated solvents, Polymer (Submitted) (n.d.).
[57] M. Nerkar, J.A. Ramsay, B.A. Ramsay, M. Kontopoulou, R.A. Hutchinson, Determination of Mark-Houwink parameters and absolute molecular weight of medium-chain-length poly(3-hydroxyalkanoates), J. Polym. Environ. 21 (2013) 24–29, https://doi.org/10.1007/s10924-012-0525-3.
[58] M.R. Kasaai, Calculation of Mark–Houwink–Sakurada (MHS) equation viscometric constants for chitosan in any solvent–temperature system using experimental reported viscometric constants data, Carbohydr. Polym. 68 (2007) 477–488, https://doi.org/10.1016/j.carbpol.2006.11.006.
[59] C. Malengreaux, Rheology and Thermal Stability of Polyhydroxyalkanoates, Lund University, Lund, 2008.
[60] L.A. Utracki, M.R. Kanial, Melt rheology of polymer blends, Polym. Eng. Sci. 22 (1982) 96–114, https://doi.org/10.1002/pen.760220211.
[61] L.A. Utracki, Melt flow of polymer blends, Polym. Eng. Sci. 23 (1983) 602–609, https://doi.org/10.1002/pen.760231103.
[62] Q. Liao, I. Noda, C.W. Frank, Melt viscoelasticity of biodegradable poly(3-hydroxybutyrate-co-3-hydroxyhexanoate) copolymers, Polymer (Guildf). 50 (2009) 6139–6148, https://doi.org/10.1016/j.polymer.2009.10.049.
[63] S. Andjelić, R.C. Scogna, Polymer crystallization rate challenges: the art of chemistry and processing, J. Appl. Polym. Sci. 132 (2015), https://doi.org/10.1002/app.42066.
[64] C. Vanheusden, J. Vanminsel, N. Reddy, P. Samyn, J. D'Haen, R. Peeters, A. Ethirajan, M. Buntinx, Fabrication of poly(3-hydroxybutyrate-co-3-hydroxyhexanoate) fibers using centrifugal fiber spinning: structure, properties and application potential, Polymers (Basel) 15 (2023) 1181, https://doi.org/10.3390/polym15051181.
[65] C.H. Lee, S.H. Lee, A. Khalina, S.M. Sapuan, R.A. Ilyas, Development and processing of PLA, PHA, and other biopolymers, Adv. Proc. Propert. Appl. Starch Other Bio-Based Polymers (2020) 47–63, https://doi.org/10.1016/B978-0-12-819661-8.00005-6.
[66] M.M. Cross, Rheology of non-Newtonian fluids: a new flow equation for pseudoplastic systems, J. Colloid Sci. 20 (1965) 417–437, https://doi.org/10.1016/0095-8522(65)90022-X.
[67] W. Richtering, Understanding rheology, Appl. Rheol. 12 (2002) 233, https://doi.org/10.1515/arh-2002-0030.
[68] J.M. Dealy, K.F Wissbrun. Melt rheology and its role in plastics processing: theory and applications, Springer Netherlands, Dordrecht, 1999, https://doi.org/10.1007/978-94-009-2163-4.
[69] J.G. Mallette, R.R. Soberanis, Evaluation of rheological properties of non-newtonian fluids in internal mixers: an alternative method based on the power law model, Polym. Eng. Sci. 38 (1998) 1436–1442, https://doi.org/10.1002/pen.10314.